Mass transport studies in the growth of cdTe crystals by multi-tube physical vapour transport

Nicholas Maclaren Aitken

Mass Transport Studies In The Growth Of CdTe Crystals By Multi-Tube Physical Vapour Transport

By

Nicholas MacLaren Aitken

A Thesis Presented in Candidature for the Degree of

Master of Science

in the

University of Durham

UK

Department of Physics

September 1999

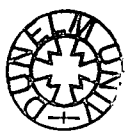

Abstract

This thesis covers some of the development of a novel vapour growth system for the production of large, high quality crystals of cadmium telluride, focusing in particular on ampoule development, flow calibration, and mass transport studies.

The Multi Tube Physical Vapour Transport system is an evolution of the Markov design, the unique feature being a U-Tube ampoule configuration which allows direct viewing of the crystal surface, and in-situ, non invasive vapour pressure monitoring. The system incorporates a capillary flow restrictor between source material and the growing crystal which allows the mass transport rate to be controlled almost independently of crystal temperature.

The growth tube section of the ampoule has been modified to allow hardened platinum wires of well defined diameter to be inserted between the crystal holder (a conical plug with polished upper surface which fits into a ground glass socket in the growth tube) and ampoule wall, allowing the annulus gap to be defined by the thickness of the wire.

A shielding system for the vapour pressure monitoring system has been developed and tested which prevents cadmium or cadmium telluride (which has escaped from the growth ampoule via non perfect ground glass joints) from condensing on the sapphire windows of the outer vacuum jacket.

The capillary flow restrictor has been calibrated for viscous, molecular and mixed flow regimes using several test gasses. This information has been used to model the mass transport of CdTe in 3 growth runs of the MTPVT system by integrating viscous and molecular flow rates with respect to time. The mass of CdTe transported from source to crystal during each run selected for study was in good agreement with the mass transport of CdTe predicted by the flow model.

Declaration

I declare that all the work in this thesis was carried out by the candidate except when explicitly stated otherwise. I also declare that none of this work has been previously submitted for any other degree.

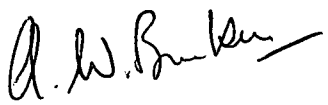

Dr A. W. Brinkman

Supervisor

N. M. Aitken

Candidate

Acknowledgements

Many thanks to my supervisor Dr Andy Brinkman for the opportunity to do this MSc degree and being of constant support throughout. I would also like to thank all the members of the 2-6 semiconductors and ceramics group, in particular Dr John Mullins for his invaluable help during the course of this work, and Dr Josep Carles-Alabert who was also a source of great help and whose Ph.D. thesis was the source of much of the information presented in chapter 1.

Contents

Chapter 1

Cadmium Telluride Properties and Vapour Growth Development

1.1 Introduction 2

1.2 Thermodynamic Properties of Cadmium Telluride 4

1.3 Mechanical Properties 7

1.4 Current Vapour Growth Techniques 8

References for chapter 1 14

Chapter 2

MTPVT Growth System

2.1 Introduction 17

2.2 General Design Features 17

2.3 Vacuum System 19

2.4 Heating Elements 20

2.5 Growth Ampoule 22

2.6 Vapour Pressure Monitoring 24

2.7 Computer Control 25

2.8 Growth Procedure 27

2.10 Summary 28

References for Chapter 2 30

Chapter 3

System Modifications

3.1 Introduction 32

3.2 Growth Tube Modifications 32

3.3 Vapour Pressure Monitoring System Modifications 35

References for chapter 3 42

Chapter 4

Synthesis of Cadmium Telluride Source Material

4.1 Introduction 44

4.2 Method 44

4.2.1 Material Preparation 44

4.2.2 Ampoule Preparation 45

4.2.3 Furnace Temperature Profile 46

4.3 Conclusion 48

Chapter 5

Calibration of the Crossmember Flow Restrictor

5.1 Introduction 50

5.2 The Fluid Dynamics of Capillary Flow 51

5.3 Molecular Flow 52

5.4 Viscous Flow 53

5.5 Mixed Flow 53

5.6 Compressible and Turbulent Flow 54

5.7 Room Temperature and Growth Temperature Conditions 55

5.8 Experimental Set-up 56

5.9 Results 57

5.10 Capillary Dimensions 59

5.11 Discussion and Conclusion 59

References for chapter 5 63

Chapter 6

Mass Transport in the MTPVT System

6.1 Introduction 65

6.2 Theory 66

6.3 Results and Discussion 68

6.3.1 Run 44 69

6.3.2 Run 41 73

6.3.3 Run 45 75

6.4 Conclusion 79

References for chapter 6 80

Chapter 7

Conclusion and Suggestions For Further Work 82

References for Chapter 7 84

Appendix 1 85

Appendix 2 86

Chapter 1

Cadmium Telluride Properties and Vapour Growth Development

Chapter 1

Cadmium Telluride Properties and Vapour Growth Development

1.1 Introduction

The binary 2-6 semiconductor cadmium telluride has applications in several technologically important areas. The first major application of the material was as a substrate for the epitaxial growth of mercury cadmium telluride, $Hg_{1-x}Cd_xTe$, an important material with tuneable bandgap, with applications in the field of infra red detection (*ref 1*). Cadmium telluride has been replaced by the more suitable substrate $Cd_{1-x}Zn_xTe$ where x is about 0.04, as this is lattice matched to important compositions of $Hg_{1-x}Cd_xTe$. Despite the reduction in demand for substrate material, high quality bulk crystals of cadmium telluride are in increasing demand in the field of room temperature X and γ-ray radiation detection. The high electro-optical constant of CdTe has also raised interest in the field of optoelectronics, with a view to its use as a component of optical memory.

The greatest flaw in the above applications is the lack of large (>50mm diameter), high quality (dislocation densities of $< 10^4$ cm^{-2}, low concentrations of small inclusions, twin free) wafers of highly resistive and uniform CdTe. The current source of commercially available single crystals of CdTe and $Cd_{1-x}Zn_xTe$ are grown from the melt, typically by Bridgeman growth or gradient freezing techniques, where small crystals must be mined from the boule which will typically be highly twinned and multigrained. Although some melt grown boules have shown promise, results are still

inconsistent, due mainly to the thermodynamic and mechanical properties of the material.

Growth of CdTe from the vapour phase, in theory, overcomes some of the physical constraints suffered in growth from the melt. In practice however, the reproduction and accurate and precise control of crystal growth conditions presents many technical challenges, and to date no system has produced material of the required specification on a repeatable basis. This thesis describes the development of several aspects of a novel "semi-open" vapour growth system incorporating a flow restrictor between source material and crystal, with the aim of improving the control and measurement of important vapour growth parameters.

This thesis describes some of the development and calibration of a novel vapour growth system known as the *M*ulti *T*ube *P*hysical *V*apour *T*ransport (MTPVT) system which has been developed in Durham.

Chapter 1 describes the important technological applications, along with the mechanical and thermodynamic properties of cadmium telluride, before giving a brief history of the development of vapour growth and its advantages over melt growth techniques.

Chapter 2 provides an overview of the MTPVT system and general growth procedure, along with detailed descriptions of the important components of the system.

Chapter 3 describes modifications made to the MTPVT system during the course of this MSc. project, including changes to the growth ampoule and the vapour pressure monitoring arrangement.

Chapter 4 details production of the high purity, polycrystalline, CdTe source material from its constituent elements.

Chapter 5 covers the calibration of vapour flow rate through the capillary tube, which is incorporated into the growth ampoule and acts as a flow restriction between the source material and growing crystal.

Chapter 6 takes the calibration data from chapter 5 and compares it with measured mass transport over the course of three runs of the MTPVT system in an attempt to quantify mass flow rates based on vapour pressure measurement and temperature profile.

Chapter 7 concludes this thesis and suggests areas for further work.

1.2 Thermodynamic Properties of Cadmium Telluride

1.2.1 Temperature vs. Composition

The relationships between the vapour and solid phases of cadmium telluride with respect to temperature, pressure and composition are of vital importance to the growth procedure. Although the temperature-composition (T-x) diagram for CdTe appears characteristic of that for a binary 2-6 compound, indicating that Cd and Te_2 vapours sublime stoichiometrically at any temperature given a stoichiometric source (see fig 1.1) (*ref 2*). Closer inspection of the solidus line however reveals an asymmetric region of homogeneity (see fig 1.2) (*ref 3*). It can be seen that on sublimation at higher temperatures the vapour will be tellurium rich, resulting in an increased chance of tellurium precipitates and inclusions in the growing crystal. This effect can be minimised by using a cadmium rich source, or fixing the cadmium pressure by using a high purity cadmium reservoir at a well defined temperature. In practice however the easiest way to achieve a stoichiometric crystal is to keep the temperature of the growing crystal as low as possible.

Fig 1.1 Temperature - composition diagram for CdTe

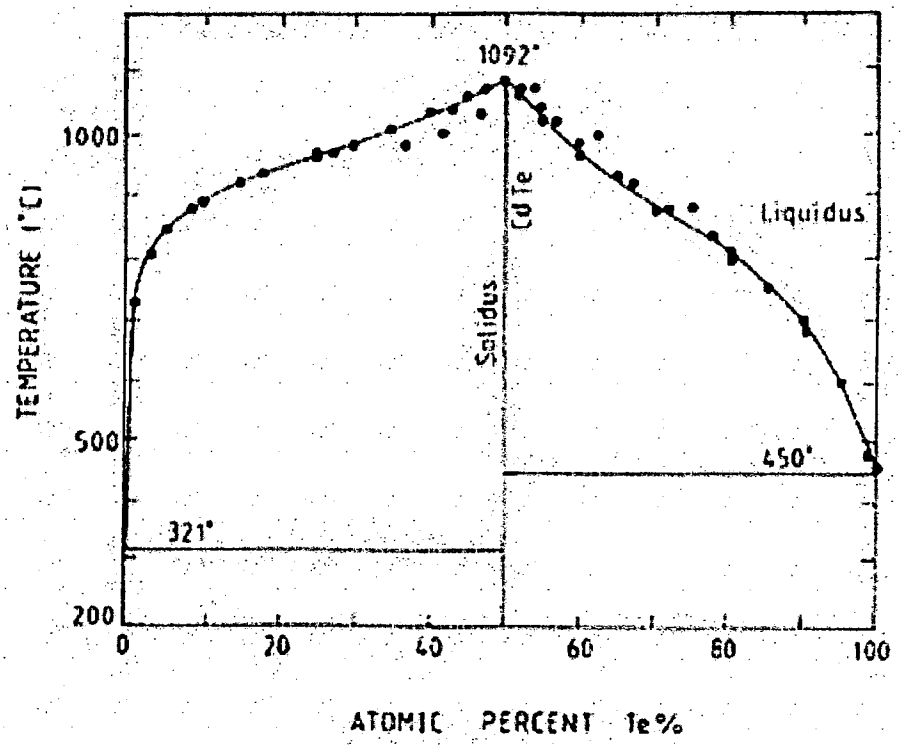

Fig 1.2 T-x projection of CdTe diagram

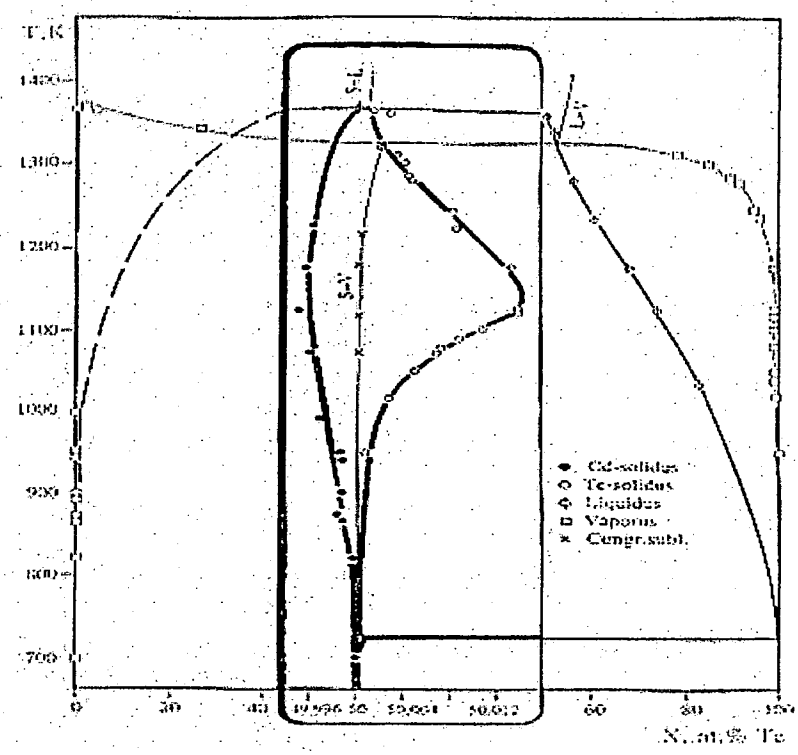

1.2.2 Pressure vs. Temperature

The equilibrium reaction for the heating of cadmium telluride is given by *eq 1.1.*

$$CdTe_{(s)} \Leftrightarrow Cd_{(g)} + \frac{1}{2}Te_{2(g)} \qquad eq\ 1.1$$

This equation is somewhat an approximation as there should be a correction term for defect concentrations and any excess component.

The mass action law which corresponds to this reaction is given by

$$K_{CdTe}(T) = P_{Cd}P_{Te_2}^{1/2} = e^{\frac{\Delta G}{RT}} \qquad eq\ 1.2$$

Where R is the gas constant, ΔG is the free energy of formation and $K_{CdTe}(T)$ is the equilibrium constant of the reaction and P_{Cd} and P_{Te2} are the partial vapour pressures of cadmium and tellurium respectively.

From *eq 1.1*:-

$$P_{Cd} = 2P_{Te_2} \qquad eq\ 1.3$$

for a small volume of CdTe subliming into a relatively larger ampoule, which is a significant constraint in closed ampoule growth.

Due to the approximation of *eq 1.1* it follows that *eq 1.2* will therefore be slightly concentration dependent.

By measuring the absorption of light passing through Cd and Te_2 vapour over congruently subliming CdTe, (where the vapour was stoichiometric to better than 10^{-3} at.%, the maximum deviation from stoichiometry in the solid) in the temperature range 780-939 °C, the relations in *eq 1.4* and *eq 1.5* were obtained (ref 4).

$$\log P_{Cd}\,(\text{mbar}) = -\frac{1\times10^4}{T} + 9.351 \qquad eq\ 1.4$$

$$\log P_{Te2}\,(\text{mbar}) = -\frac{1\times10^4}{T} + 9.652 \qquad eq\ 1.5$$

Combining *eq 1.4* and *eq 1.5* with *eq 1.2* gives the free energy of formation and equilibrium constant, *eq 1.6* and *1.7* respectively.

$$\Delta G\left(\frac{Kcal}{mol}\right) = -68.64 + 44.94\times10^{-3}T \qquad eq1.6$$

$$\log K_{CdTe}(mbar^{3/2}) = -\frac{1.5\times10^{4}}{T} + 14.177 \qquad eq\ 1.7$$

1.3 Mechanical Properties

Cadmium telluride is an intrinsically brittle and mechanically weak substance at all temperatures, with low stacking fault energy and critical shear stress (*ref 5,6*). This means small stresses applied to the growing crystal can cause defects, and these defects will propagate and multiply easily through the lattice, compared to other typical semiconductor materials. The critical resolved shear stress for CdTe has been measured with respect to temperature (*ref 5*) and falls from 5MPa at room temperature to approximately 0.2 MPa approaching the melting point of 1092°C. This again emphasises the advantage of growing the crystal at as low a temperature as possible.

Elimination of stress applied to the growing crystal is essential in the production of high quality material, the principle causes of stress on the crystal being the interaction of the boule with the walls of the ampoule and the crystal support, and thermal stress caused by radial temperature gradients across the crystal, especially during the cooling process. The linear thermal expansion coefficient of CdTe has been measured by several authors and is approximately a constant 5.3×10^{-6} °C^{-1} over the temperature range 20-800 °C (*ref 6*), where as that of silica (the ampoule material of choice) is 5.5×10^{-7} °C^{-1}. Due to oxide layers unavoidably present on the CdTe surfaces,

specifically CdO and TeO_2, there is normally some degree of adhesion, or wetting, between the CdTe and ampoule walls (*ref 7,8*), resulting in tensile stress being applied to the crystal during the cooling process. It has also been shown that a radial temperature differences of just 2 °C within the crystal can cause thermal stress higher than the critical resolved shear stress (*ref 9*).

1.4 Current Vapour Growth Techniques

The majority of single crystal CdTe is currently cut from large boules (up to 100 mm diameter) of CdTe grown from the liquid phase, predominantly produced using gradient freezing or modified Bridgman techniques. The principle drawbacks of melt growth are the low thermal conductivity, critical resolved shear stress, and stacking fault energy of CdTe. A further complication is the non stoichiometric vapour pressure above the CdTe melt, leaving a tellurium rich melt if the vapour pressure is not controlled in some way.

As CdTe has a relatively high vapour pressure below its melting point this allows vapour growth to take place at lower temperatures, giving a theoretical reduction in precipitates, inclusions and defects (due to the lower thermal stresses applied to the crystal and higher critical resolved shear stress at lower temperatures). Vapour growth also has a purification action, in that non volatile impurities are not transported from source to crystal.

The principal problems associated with vapour growth concern non stoichiometric sublimation of the source material and the control thereof, control of the mass transport rate, and control of seeding in certain systems, making reproducibility or results and conditions difficult with existing technologies.

There are two principle modes of vapour growth, closed vapour growth and semi-open vapour growth. The former normally being conducted in a sealed ampoule and the latter in an unsealed ampoule under dynamic vacuum, or possibly in a stream of inert gas.

Closed vapour growth methods were first used by Czyzac (*ref 10*) and subsequently developed by Piper and Polich (*ref 11*) for CdS. This is an unseeded method, where the ampoule is tapered to a conical tip which acts as a nucleation point. The charged ampoule is placed in a suitable temperature gradient where vapour is transported to the conical tip and self seeding takes place. The ampoule need not necessarily be sealed before growth as the condensing vapours will seal the ampoule. This eliminates gasses produced during the sealing process and also allows some outgassing of the source material during the heating process.

One important development of the Piper and Polich method was the introduction of an elemental reservoir of well defined temperature independent of the ampoule temperature (*ref 12*). This fixes the vapour pressure of one of the elements, typically cadmium, and as can be seen from the mass action law of *eq 1.2* this will create a stoichiometric vapour. This method was employed by the Durham group who used an arrangement shown in *fig1.3* (*ref 13,14*), however the transport rates were often very low with growth taking place over up to two to three weeks to grow a boule of ~30cm^3 which was multigrained and twinned. The low growth rates achieved by closed vapour growth are attributed to diffusion barriers, either due to impurities introduced during sealing or from outgassing of the source. More significantly diffusion barriers are also set up in the non stoichiometric vapour, where typically tellurium excess will reduce growth rates, as reported by Rosenberger (*ref 15, 16*).

The above limitations lead to generally low product quality, and poor repeatability of

results due to the large uncertainty introduced by the sealing process and non perfect source material.

Fig 1.3 Closed CdTe vapour growth, incorporating elemental reservoir.

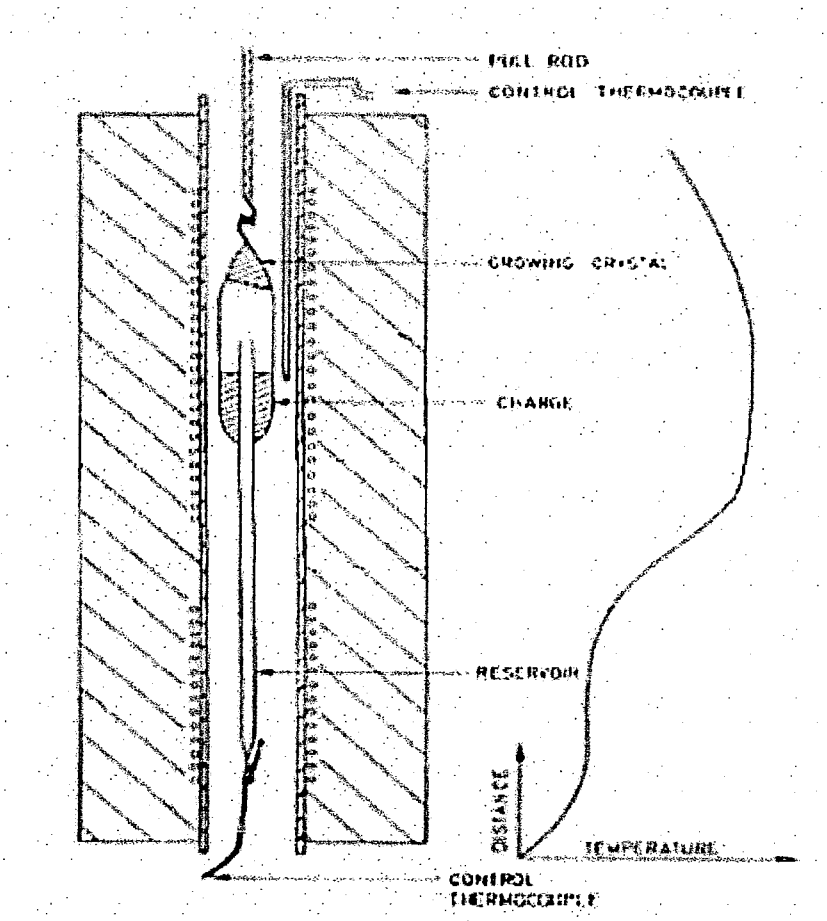

Semi-open vapour growth has several advantages over closed ampoule growth, growth rates can be up to three orders of magnitude higher than the closed ampoule equivalent, and this allows growth temperatures to be reduced closer to the region of homogeneity (see section 1.2.1). It is possible to avoid contact of the growing crystal with the ampoule walls which was a significant limitation associated with closed ampoule growth, and volatile impurities introduced by the source material

diffuse out of the ampoule, reducing the possibility of incorporation into the growing crystal and reducing the growth limiting diffusion barriers which they may create.

The "nearly closed" method of vapour growth, where initially unsealed ampoules were sealed by the growing crystal, as used by Piper and Polich for the growth of CdS crystals (*ref 11*) and subsequently quantified by Factor et al (*ref 17, 18, 19*), was followed by the introduction of effusion holes in the ampoule walls, allowing continuous evacuation of the ampoule, which was surrounded by a dynamic vacuum, or in some cases a known pressure of one of the growth elements or an inert gas. This creates a stable vapour pressure within the ampoule and consequently increases growth rates by reducing diffusion barriers, precipitate and inclusion density is also reduced.

Another important development, first used by Rosenberger et al (*ref 20*) for the growth of KCl and KBr crystals, was the removal of the growing crystal from contact with the ampoule walls, eliminating the wetting effects which impose considerable stress on the crystal, especially during the cooldown process. It was Markov and Davydov (*ref 21, 22*) who developed semi open growth for 2-6 compounds. In their method a seed was supported on a silica rod in a vertical ampoule tube. The arrangement was such that there was a small annular gap between the silica rod and the walls of the ampoule, thus allowing excess material and volatile impurities to diffuse past the growing crystal to a cold sink region below the silica rod (see fig 1.4). In some systems the silica rod also acts as a heat pipe, (*ref 23*) conducting heat away from the crystal and creating a sharper temperature gradient just above the crystal vapour interface, thus encouraging condensation of vapours onto the seed. This

method has been successful in producing twin free crystals of up to 100mm in diameter, however the heat pipe restricts the height of growth to about 10 mm. The latest advance in ampoule design has been the incorporation of a capillary or similar flow restriction between charge and seed, allowing the mass transport rate to be controlled almost independently of crystal temperature, as reported by Rosenberger (*ref 7*). It is this generation of the Markov design which has produced material with the lowest reported etch pit density, 2×10^3 cm^{-2}. The decoupling of source temperature and crystal temperature allows the most versatile growth procedures, where the growing crystal can be maintained at the most favourable temperature for stoichiometric

Fig 1.4 Markov design of semi - open growth system.

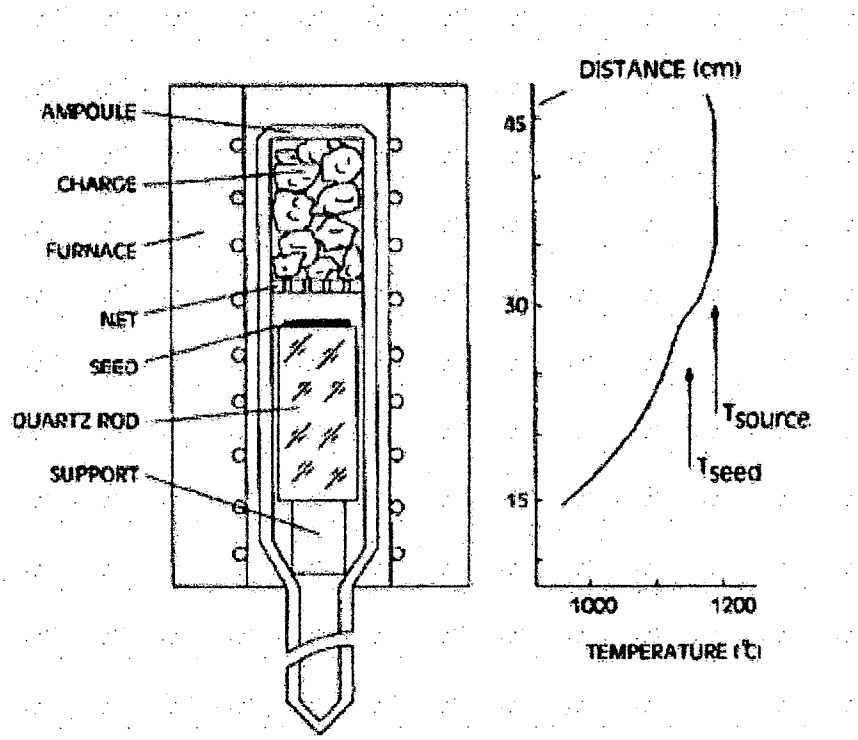

growth, while the growth rate can be set by the source temperature to be kinetically (or commercially) favourable. It is the development of this generation of vapour growth system for the production of cadmium telluride which is the subject of this thesis.

References for chapter 1

1. Narrow gap 2-6 compounds for Optoelectronic and Electromagnetic Applications, Electronic Materials Series, vol 3, Edited by P Capper, pub. Chapman & Hall, London (1997)
2. M. Hage-Ali and P. Siffert, Growth Methods of CdTe Nuclear Detection Materials, in Semiconductors for Room Temperature Nuclear Detectors Applications, vol 43, Edited By T. E. Schlesinger and R. B. James, pub Academic Press, San Diego (1995)
3. J. H. Greenberg, P-T-X Phase Equilibrium and Vapour Pressure Scanning of Non-Stoichiometry in CdTe, J. Crystal Growth, 161 (1996) 1
4. R. F. Brebrick and A.J. Strauss, Partial Pressures and Gibbs Free energy of formation for Congruently Subliming CdTd, J. Phys. Chem. Solids, 25 (1964) 1441
5. R. Balasubramanian and R. W. Wilkox, Mechanical Properties of CdTe, Mat. Sci. Eng, B16 (1993) 1
6. H. Hartmann, R. Mach and B. Selle, Wide Gap 2-6 Compounds as Electronic Materials, in Current Topics in Materials Science, vol 9, Edited by E. Kaldis, North-Holland, Amsterdam (1982)
7. F. Rosenberger, M. Banish and M. B. Duval, Vapour Crystal Growth Technology Development- Application to Cadmium Telluride, NASSA Technical Memorandum 103786 (1991)
8. R. K. Bagai, R. D. S. Yadava, B. S. Sundersheshu, G. L. Seth, M. Anandad, W. N. Borle, A Study on Contaminations During Bulk Growth of CdTe Crystals, J. Crystal Growth, 139 (1994) 258
9. J. C. Alabert, Optical Vapour Pressure Monitoring and Mass Transport Control During Bulk CdTe Crystal Growth in a Novel Multi Tube PVT System, Appendix A, Ph.d. Thesis, University of Durham, UK, (1998)
10. S. J. Czyzak, D. G. Craig, C. E. McCain and D. W. Reynolds, Single Synthetic Cadmium Sulphide Crystals, J. App. Phys.,23 (1952) 932
11. W. W. Piper and S. J. Polich, Vapour Phase Growth of Single Crystals of 2-6 Compounds, J. App. Phys., 32 (1961) 1278

12. P. Hoschl and C. Konak, Sublimation of Cadmium Telluride and Cadmium Selenide under a Vapour pressure of their Components and the Equilibrium Form of Crystal Growth, Phys. Stat. Sol. 9 (1965) 167

13.. J. R. Cutter The Crystal Growth and Properties of Some Chalcogenides of Zink and Cadmium, Phd Thesis, University of Durham, UK (1977)

14. K. Durose, G. J. Russell and J. Woods. Structural Properties of Crystals of CdTe Grown from the Vapour Phase, J. Crystal Growth, 72 (1985) 85

15. D. W. Greenwell, B. L. Markham and F. Rosenberger, Numerical Modeling of Diffusive Physical Vapour Transport in Cylindrical Ampoules, J. Crystal Growth, 51 (1981) 413

16. F. Rosenberger, J. Ouazzani, I. Viohl and N. Buchan, Physical Vapour Transport Revisited, J. Crystal Growth, 171 (1997) 271

17. M. M. Faktor, R. Heckingbottom, I. Garret, Growth of Crystals form the Gas Phase part 1. Diffusional Limitations and Interfacial Stability in Crystal Growth by Dissociative Sublimation, J. Chem. Soc A (1970) 1257

18. M. M. Faktor, R. Heckingbottom and I. Garret, Growth of Crystals form the Gas Phase part 2. Diffusional Limitations and Interfacial Stability in Crystal Growth by Dissociative Sublimation, with an Inert Third Gas Present, J. Chem. Soc A, (1971) 1

19. M. M. Faktor, R. Heckingbottom and I. Garret, Diffusional Limitations in Gas Phase Growth of Crystals, J. Crystal Growth, 9 (1971) 3

20. F. Rosenberger, G. H. Westphal, Low Stress Physical Vapour Growth (PVT), J. Crystal Growth, 43 (1978) 148

21 E. V. Markov and A. A. Davydov, Sublimation of CdS Crystals, Inorg Matter 7 (1971) 503

22. E. V. Markov and A. A. Davydov, Growth of Oriented Monocrystals of CdS from the Vapour Phase, Inorg. Matter 11 (1975) 1504

23. H. Kuwamoto, Seeded Growth of Large Single Grain CdTe from the Vapour Phase, J. Crystal Growth, 69 (1984) 204

Chapter 2

MTPVT Growth System

Chapter 2

MTPVT Growth System

2.1 Introduction.

The crystal growth system is essentially a combination of the Rosenburger capillary restricted transport and Markov designs (*ref 1,2*), and was initially developed by Dr J. T. Mullins (*ref 3*). The important differences and improvements over the Markov design are the U-Tube configuration. This chapter will describe the main elements of the growth system.

2.2 General Design Features.

A schematic diagram of the system is shown in *fig(2.1)*. In essence, the growth system comprises two quartz tubes, for source charge and growth sink, connected by a quartz crossmember with a capillary flow restrictor. Two three zone furnaces heat the source and growth tubes, the crossmember is optically heated by two 1 kW lamps. The entire assembly is housed in a stainless steel evacuated chamber, which provides thermal isolation for the growth ampoule, as well as secure containment during growth.

Fig 2.1

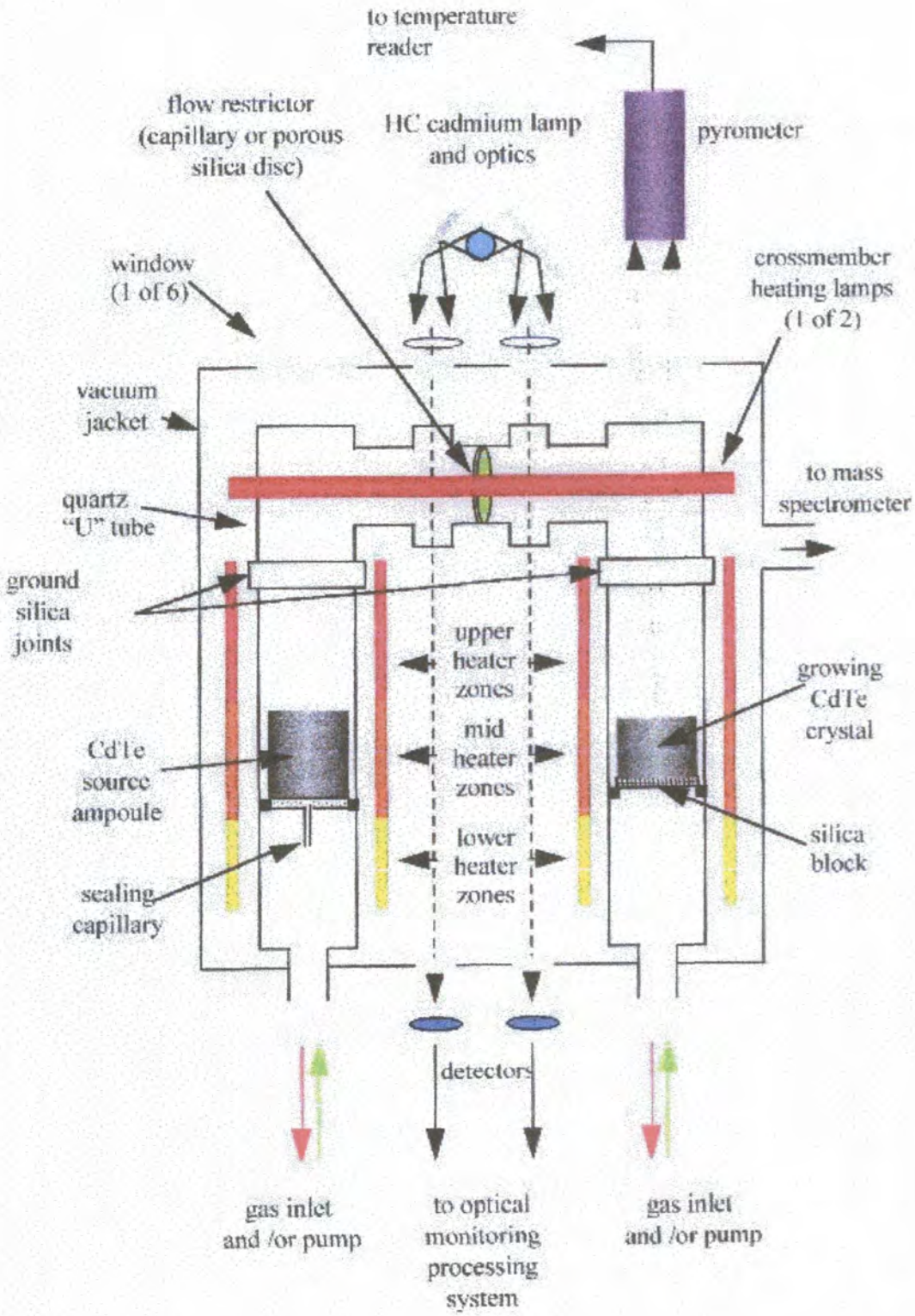

Schematic Design of the Multi-Tube Physical Vapour Transport (MTPVT) System.

2.3 Vacuum System.

The vacuum system comprises a stainless steel cylinder with stainless steel base and top plates which are sealed with rubber O-rings. The base plate, which supports the furnaces, is lowered on screw threads to provide access to the system, it also contains several feed through connections to provide power for the furnaces and heating lamps, along with thermocouple connections.

The main chamber is evacuated using a turbomolecular pump and typical pressures of $10^{-6} \sim 10^{-8}$ mbar can be achieved after baking the system out for 24 hours. This outer vacuum jacket is dynamically pumped and provides the continuous pumping for the growth ampoule via a valve connected to the bottom of the sink tube. There is also the facility to evacuate the ampoule independently via a valve at the bottom of the source tube, which is connected, to an external rotary pump. The ability to evacuate the ampoule before pumping the main chamber is important in order to protect against any sudden reduction in pressure as the turbo pump starts, potentially dislodging the ground glass joints of the ampoule.

The top and bottom plates incorporate two 15mm diameter UHV sapphire windows, which allow light from a cadmium lamp to be passed through the vapour on the source and sink sides of the crossmember flow restrictor respectively. This arrangement allows source and sink vapour pressure to be determined as described in section 2.6. In addition, the top plate has two larger sapphire windows to allow observation of, and pyrometric measurements to be made on, the growing crystal and source charge. During growth, there is a small loss of CdTe through the ground glass joints of the ampoule, typically <1%. Two 16mm diameter quartz tubes with one end sealed by 15mm polished quartz discs lead from the outer windows to as close as

possible to windows in the crossmember in order to prevent CdTe from condensing on the outer vapour pressure monitoring windows, which are cold spots.

A mass spectrometer is attached through the top plate and this acts as a leak detector by way of ensuring there is no oxygen present. It also provides information on any volatile impurities in the system throughout bakeout and growth, although the presence of any Cd or Te_2, due to escape through the ground glass joints of the ampoule, can not be detected as it will have condensed before reaching the spectrometer.

2.4 Heating Elements

The two three zone furnaces which heat the source and growth tubes consist of pyrolytic boron nitride insulating tubes with graphite windings. Contacts are made with high purity, low copper content contact blocks. Each zone can be independently computer controlled. The use of three zones in the source side allows a temperature profile which maintains the source at an approximately uniform temperature whilst leaving the base of the tube cooler, thus allowing the capillary at the bottom of the source tube to be sealed if no gas flow has been introduced (see section 2.5). On the growth side this allows, in principle, the selection of an advantageous radial temperature profile across the growing surface, especially if fine-tuned using pyrometry.

Two quartz halogen lamps are used to heat the crossmember. This radiative heating mechanism allows the in-situ, non-destructive vapour pressure monitoring and pyrometric crystal surface temperature measurement. The lamps are controlled independently of the zone furnaces and ideally provide an isothermal crossmember. As was shown by thermal modelling of the system, (using I-DEAS^{TM} thermal modelling software) cold spots arise due to the viewing and vapour pressure

monitoring windows. In an effort to minimise this, and keep the outer jacket at a safe temperature (<100^{0}C), stainless steel and molybdenum heat shields surround the crossmember and source and growth tubes *see fig(2.2).* The outer jacket is water cooled as a further safeguard.

Seven Pt/Pt13%Rh thermocouples measure the temperature of each furnace zone and the crossmember temperature with an accuracy of ~ 1^{0}C and stability of ~0.1^{0}C. Thermocouple voltages are multiplexed and measured by a digital voltmeter, which is PC controlled.

fig 2.2

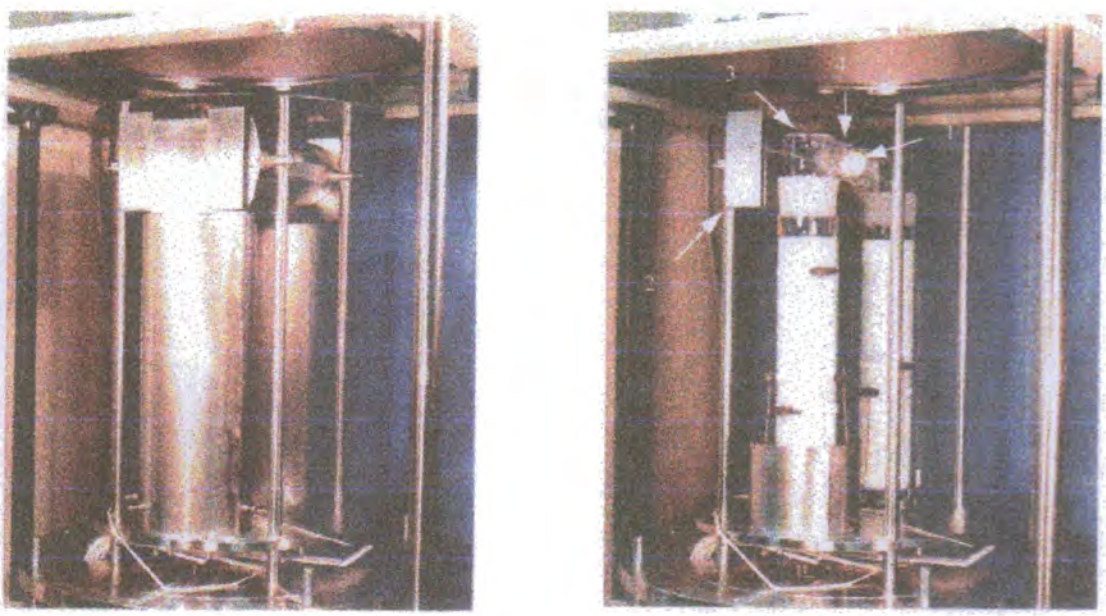

Interior of the MTPVT system with and without heat shields. note:- 1, flow restrictor (earlier sinter design) 2, one of the quartz halogen heating lamps with heat shielding 3, growth side viewing window 4, vapour pressure monitoring windows

2.5 Growth Ampoule

The ampoule comprises two quartz tubes of 49mm maximum inner diameter, connected by ground glass joints to the quartz crossmember. The ampoule is dynamically pumped from the bottom of the growth tube, through the valved opening to the outer chamber. To date, two designs of growth tube have been used. In the case of the first arrangement, there is a gap of ~50μm between the silica block and quartz wall of the tube. In this classic Markov type arrangement, a 49mm seed sits on a 49mm silica block, typically 1-5 cm in length. This rests on three permanent indentations in the wall of the tube. In the second arrangement, a 29mm seed sits on a quartz plug, which fits into a conical ground glass joint of approximately 3 cm in length. A gap between the plug and glass joint is defined by inserting hardened, high purity platinum wires of calibrated diameter, (typically between 25μm and 150μm) between the two. The narrow gap between crystal pedestal (and seed) and ampoule wall results in continuous removal of excess components, as well as any volatile impurities from the source material, away from the growing surface, greatly improving crystal purity and stoichiometry, (*ref 4*), it also helps to prevent the crystal from sticking to the ampoule as in closed ampoule techniques.

The source tube is connected to the "outside" by a capillary at the bottom of the source tube. This enables the ampoule to be evacuated before pumping of the main chamber begins, it also allows for the introduction of a constant gas flow either before or during growth to act as a reducing agent and/or to preserve the integrity of the seed, although this has yet to be implemented. If no gas flow is introduced then CdTe seals the capillary during the initial sublimation period due to the lower temperature of this region than the source material.

Typically, about 500g of high purity, polycrystalline, CdTe is placed in the growth tube at the middle heating zone (the production of which is detailed in chapter 4). This is sufficient material to grow several crystals, and once in place is not replaced until nearly exhausted.

The crossmember has three main features. Firstly it houses the capillary flow restrictor (calibration of which is detailed in chapter 5). This is approximately 1.5 cm in length and 1 mm in diameter. The original crossmember design incorporated a porous sinter disc as a flow restrictor, however this proved to reduce transport rates too much, especially from a commercial point of view. The effect of the restrictor is to allow a further decoupling of the source and growth temperatures. Flow through the capillary is a function of pressure drop between source and sink, rather than temperature difference (*ref 7*). This allows the seed to be maintained in a temperature range where the homogeneity region for CdTe is narrow (*ref 5*) while maintaining high transport rates.

Secondly, there is a polished quartz window above the growth tube to provide optical access to the growing surface. This allows observation of the nucleation process during growth, and, in principal, pyrometric measurements to be made across the growing surface see *fig (2.3)*. Originally, there was an identical window above the source tube however, this was sacrificed in favour of structural strength.

Thirdly, there are two 15 mm diameter polished quartz sections, which provide a transverse optical path through the vapour. This allows optical monitoring of the vapour pressures on source and growth sides of the system by measuring absorption of light from a cadmium lamp.

Fig 2.3 Photograph of CdTe crystal during growth in the MTPVT system.

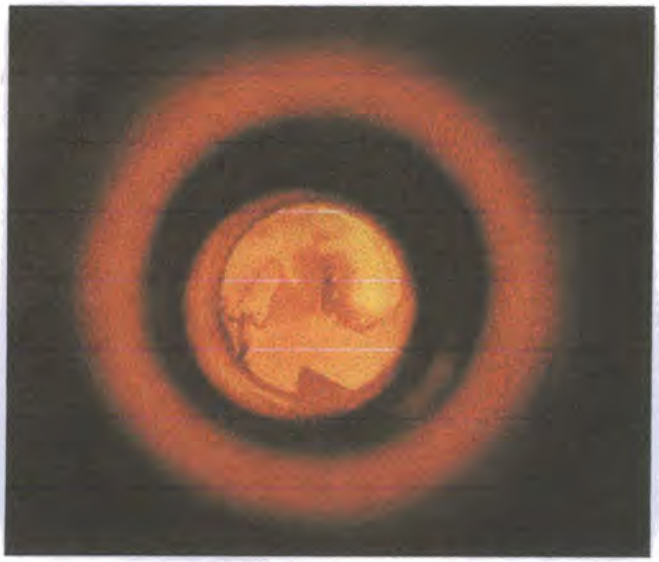

2.6 Vapour Pressure Monitoring.

The experimental arrangement for vapour pressure measurement is shown in *fig(2.4)*. The light source is a cadmium hollow cathode lamp with Pyrex envelope. This has a spectrum of very narrow emission lines. These include a 326.1nm line which is absorbed by cadmium vapour, a 508 nm line which is absorbed by the broad band, molecular absorption spectrum of tellurium vapour, and a 643.8 nm line which is unaffected by either element at low pressures and is used as a reference line, (*ref 6*). Cadmium vapour has two principle absorption lines, centred at 228.7 nm and 326.1 nm, hence the 508 nm and 643.8 nm excited cadmium emission lines of the monitoring lamp are unaffected,(*ref 6*).

The detection system monitors each line on each side of the crossmember restrictor simultaneously. The detectors are silicon photodiodes (Hamamatsu S1336-18BK for the 643.8 and 508 nm lines and S1336-18BQ for the 326.1 nm line). Appropriate interference filters above each detector allow them only to detect their designated line.

The photocurrents are then amplified by operational amplifiers before being multiplexed and measured by a lock-in amplifier. The signal is then recorded by a digital voltmeter and stored by a PC.

fig (2.4) Top of MTPVT system photographed during growth:

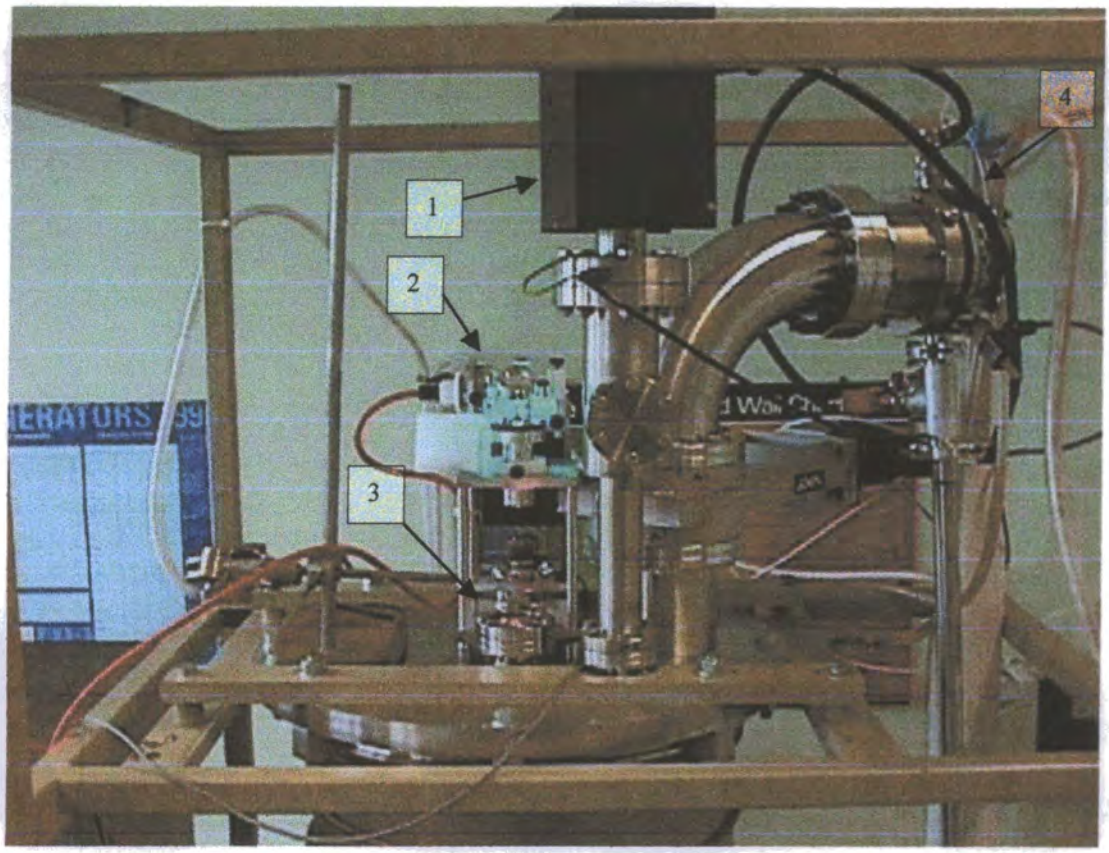

1, mass spectrometer head 2, cadmium lamp and aligning optics 3, vapour pressure and viewing windows 4, turbomolecular pump

2.7 Computer Control.

The system is PC controlled using a PASCAL program which co-ordinates the multiplexing of the vapour pressure detectors and thermocouples, see *fig (2.6)*. An IEEE interface is used to control and read a digital volt meter which measures the

thermocouple voltages and amplified photocurrents in cycles of about 1 min. This data is used to control the power supplied to each of the seven heating zones via thyristor packs. The temperature of each zone is controlled to within ~0.1^{0}C and can be ramped up or down independently at any rate within the heating capabilities of the furnaces. The program stores all temperature and vapour pressure data.

fig (2.6) Schematic diagram of MTPVT control system

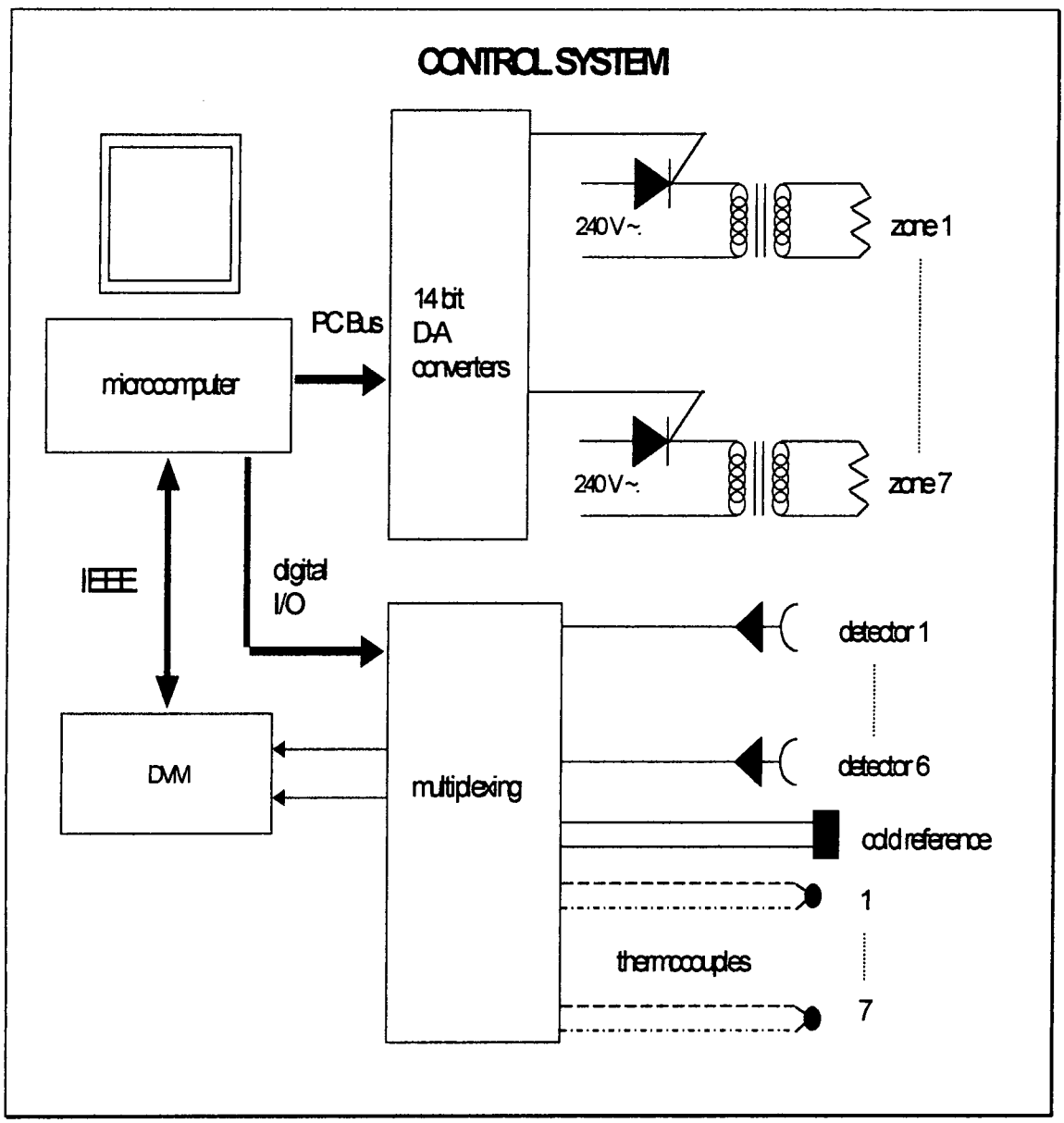

2.8 Growth Procedure.

The growth procedure has not yet been optimised and the best growth temperatures and heating profiles are still under investigation due to the large number of possibilities available.

Once the seed has been prepared, it is lowered onto the pedestal, which is already located in the growth tube. The source and growth tubes are put in place and then the crossmember fitted. Ground glass joints connect the ampoule to the two pumping systems and once these have been located the crossmember heat shields are attached and the system closed.

Firstly the ampoule is evacuated using a rotary pump and after 1 hour of pumping typical pressures of $< 10^{-1}$ mbar are achieved. Pumping of the vacuum jacket is then started using the turbo pump. Pumping continues over about 24 hours before all zones of the system are raised to 100^0C to remove volatile impurities, mainly water. After a further 24 hours the temperature is raised to 200^0C for another day before the growth run starts. Throughout bakeout, the vacuum is analysed using the mass spectrometer. At this point, the baseline vapour pressure signals are measured.

The heat shields around the crossmember are prone to differential thermal expansion and this causes an oscillation in the vapour pressure signals. To minimise this effect the temperature is ramped to growth conditions over a long period, typically up to 48 hours. Care is taken not to evaporate the seed, although some thermal etching is desirable in order to remove any oxide or bromine layer left by the chemical polishing process. With this in mind, the temperature of the growth tube is kept well below that of the source tube until there is a significant vapour pressure on the source side. Depending on temperature and transport rates growth takes place for periods of

between 12 and 48 hours. As the crystal grows the temperature of the growing interface increases with height due to the temperature difference between seed pedestal and crossmember. This ultimately results in a maximum crystal size as interface temperature approaches the source temperature, although this could be counteracted if accurate pyrometry were available to directly measure the interface temperature throughout growth.

Once growth is complete, the temperature is reduced, again over about 48 hours. This not only minimises heat shield movement but also reduces the development of stress in the grown crystal. The crossmember and top zones of the furnaces are cooled more slowly than other areas. This prevents CdTe deposit forming on the crossmember (which has a much lower thermal mass than other sections of the ampoule) and glass joints. A typical temperature profile for each heating zone is shown in *fig (2.7)*.

When at room temperature air is gradually allowed into the system and the grown crystal removed.

2.10 Summary

The Durham MVPVT system has been used successfully to grow several boules, using both of the growth tube designs detailed in section 2.5 and under different growth conditions. Growth has been carried out at source temperatures between 750^0C and 875^0C, and seed temperatures between 700^0C and 850^0C. Different heating and cooling rates have also been employed.

Structural characterisation of grown crystals has been carried out (*ref 8*).

Fig 2.7 Temperature profile during a typical growth run of the MTPVT system

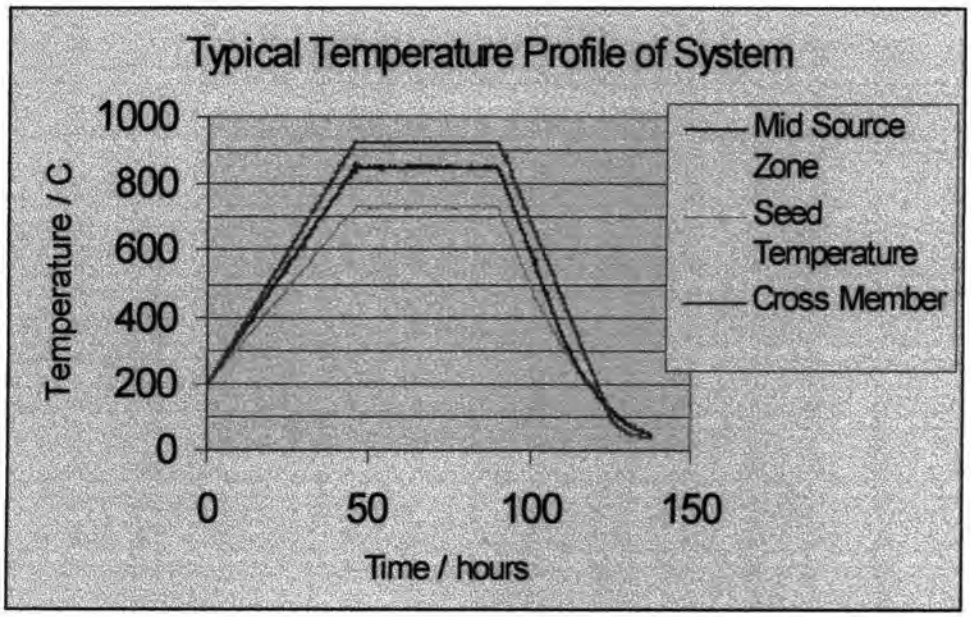

bottom and top zone temperatures are omitted for clarity

References for Chapter 2

1 E V Markov and A A Davydov, Growth of Oriented Mono Crystals of CdS From The Vapour Phase, Neo Matter. 11 (1975) 1755

2 E V Markov and A A Davydov, Sublimation of CdS Crystals, Neo. Matter. 7 (1971) 575

3 J. T. Mullins, J. Carles, N. M. Aitken and A. W. Brinkman, A Novel "Multi-tube" Vapour Growth System and it's Application to the Growth of Bulk Cadmium Telluride, accepted for publication in J. Crystal Growth

4 F Rosenberger, M Banish and M B Duval, Vapour Crystal Growth Technology Development - Application to CdTe, NASA Technical Memorandum 103786 (1991)

5 J H Greenberg P-T-X Phase Equilibrium And Vapour Pressure Scanning of Non Stoichiometry in CdTe J. Crystal Growth 161 (1996)

6 J Carles, J T Mullins and A W Brinkman, Partial Pressure Monitoring in CdTe Vapour Growth, J. Crystal Growth 174 (1997) 740.

7 J Carles, Optical Vapour Pressure Monitoring and Mass Transport Control During Bulk CdTe Crystal Growth In A Novel Multi-Tube PVT System, PhD Thesis, University of Durham, UK, (1998)

8 N M Aitken, M D G Potter, J T Mullins, J Carles, D P Halliday, K Durose B K Tanner, A W Brinkman, Characterisation of Cadmium Telluride Bulk Crystals Grown by a Novel "Multi-Tube" Vapour Growth Technique, J. Crystal Growth 198/199 (1999) 984

Chapter 3

System Modifications

Chapter 3

System Modifications.

3.1 Introduction

This chapter details recent modifications made to the MTPVT system, specifically the introduction of a new design of growth tube, and the incorporation of a heating mechanism for the vapour pressure monitoring windows.

3.2 Growth Tube Modifications.

The initial growth tube design was based on a 50 mm inner diameter tube fabricated from high purity quartz glass, into which was fitted a 49.28 mm ± 0.01 mm diameter, 10.22 ± 0.01 mm depth, ground glass pedestal to support the crystal (*see fig 2.1*). The crystal holder was supported on three indentations made in the side of the tube. The annulus gap between the crystal holder and inner wall of the tube was 0.045 mm ± 0.05 mm. The principle limitations of this design were the fixed annulus gap, preventing study of the effect of variation of the gap on growth and flow properties of the system, and the large diameter of the crystal holder, making single crystal seeds very expensive and hard to obtain. Consequently, a new growth tube was designed in an attempt to resolve both problems.

The new tube was 35mm inner diameter and featured a 30 mm maximum diameter quartz plug which fitted into a ground glass socket as a crystal holder, (*see fig 3.1*).

This design has two advantages over the first model. Firstly, the smaller diameter of the crystal holder made single crystal seeds more readily available and less expensive.

fig 3.1

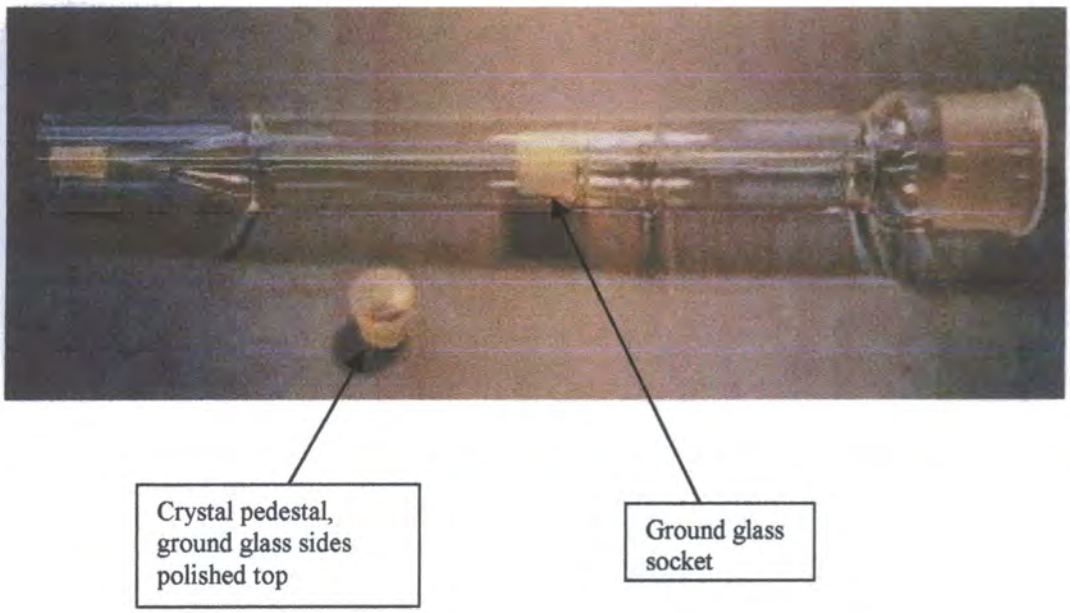

Secondly, the plug arrangement allowed the annulus gap to be varied by the insertion of hardened platinum wires between the ground glass joints of the crystal holding pedestal and growth tube.

Flow through the annulus gap can be considered entirely molecular, given that the Knudsen number, K_d, is ~ 4 for an annulus gap of 50 μm, pressure of the order of 10 mbar and temperature of 1000K, (see *sec.5.2*). The flow rate through the annulus, F_{ann}, is given by *eq 3.1* (*ref 1*).

$$F_{ann}\left[\frac{moles}{t}\right] = W \times \left(R_o^2 - R_i^2\right) \times \left(\frac{\pi}{2RT}\right)^{1/2} \times \left(\frac{\Delta P_{Cd}}{\sqrt{M_{Cd}}} + \frac{\Delta P_{Te_2}}{\sqrt{M_{Te_2}}}\right) \qquad eq\ 3.1$$

where W = transmission probability for the annulus dimensions (= 0.0419 for first

growth tube design) (*ref 2,3*), R_i and R_o are the inner and outer diameters of the annular gap respectively, M_{Cd} and M_{Te2} are the molecular masses of cadmium and tellurium vapour respectively and R is the universal gas constant.

As a first approximation it can be considered that the transmission probability, W, for the annulus gap, will scale inversely with the depth of the crystal holder, based on *eq 5.1*, and the flow rate will scale as the difference in the squares of R_o and R_I as for *eq 3.1*.

Based on this assumption and neglecting the effect of the conical shape, the approximate ratio of conductivity for the two growth tube designs, $R_{50mm}:R_{30mm} \approx 0.7$ for an annular gap of 50μm. Clearly it is necessary to calibrate gas flow past the annulus for the new design of growth tube and for each diameter of platinum wire spacers used to define the gap but it can be seen that the use of smaller diameter and longer length pedestal can be selected to give flow rates equal to those of the first design of growth tube.

An alpha step scan of the ground glass sides of the crystal pedestal was taken to give an estimate of the uncertainty in the size of the annulus gap, a plot of the scan is shown below, *fig (3.2)*.

Fig 3.2 Alpha step scan of the ground glass sides of crystal pedestal.

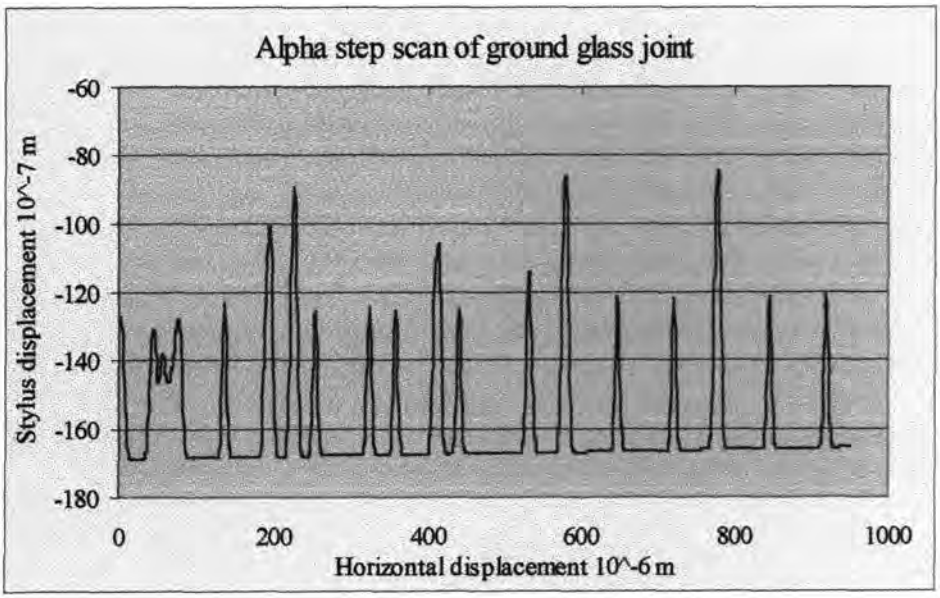

The mean width of the peak bases is 14.9 μm with a standard deviation of 3.3. The mean peak height is 5.48 μm with a standard deviation of 15.2. The mean horizontal distance from peak to peak is 54 μm. The platinum wire spacers used in initial growth runs with the new design of tube, (*see ch 6*) were 50 μm diameter. With the grains of ground glass being an average of 54 μm apart with an average height of 5.48 μm (which could be doubled considering the ground glass socket to have a similar surface to that of the pedestal) the actual annulus gap could be much smaller than intended, to the point of being a porous medium.

3.3 Vapour Pressure Monitoring System Modifications.

The ground glass joints of the growth ampoule do not provide a complete seal. Indeed when being evacuated prior to evacuation of the main chamber, the ampoule can only support a dynamic vacuum of about 10^{-1} mbar (*see sec 2.8*). The imperfect ampoule sealing results in a small loss of material to the outer vacuum jacket. Escaping

cadmium telluride will condense at cold spots in the outer jacket, specifically on the vapour pressure monitoring windows thereby compromising vapour pressure data. To prevent this it was decided to shield the windows from escaping CdTe using four lengths of 16 mm diameter quartz tube with 15 mm polished quartz discs fused to one end, leaving the other end open. The open ends were tightly fitted into the vapour pressure window flanges, although no effort was made to seal this joint. The length of the tubes was such that they came as close as possible to the vapour pressure windows on each side of the crossmember (see fig 3.3)

To determine the effectiveness of this modification, EDAX spectra were taken of the deposits found on the upper vapour pressure monitoring windows after growth runs with and without the shielding tubes in place, *figs (3.4)* and *(3.6)*, and also after a run in which there was a crack in one of the shielding tubes *fig (3.5)*. Transmission spectra through the windows, over the range of wavelengths relevant to the vapour pressure monitoring system, were also measured for the shielded and unshielded windows after a growth run, *fig (3.7)*.

Fig 3.3, schematic diagram showing the position of the shielding tubes for the vapour pressure monitoring windows.

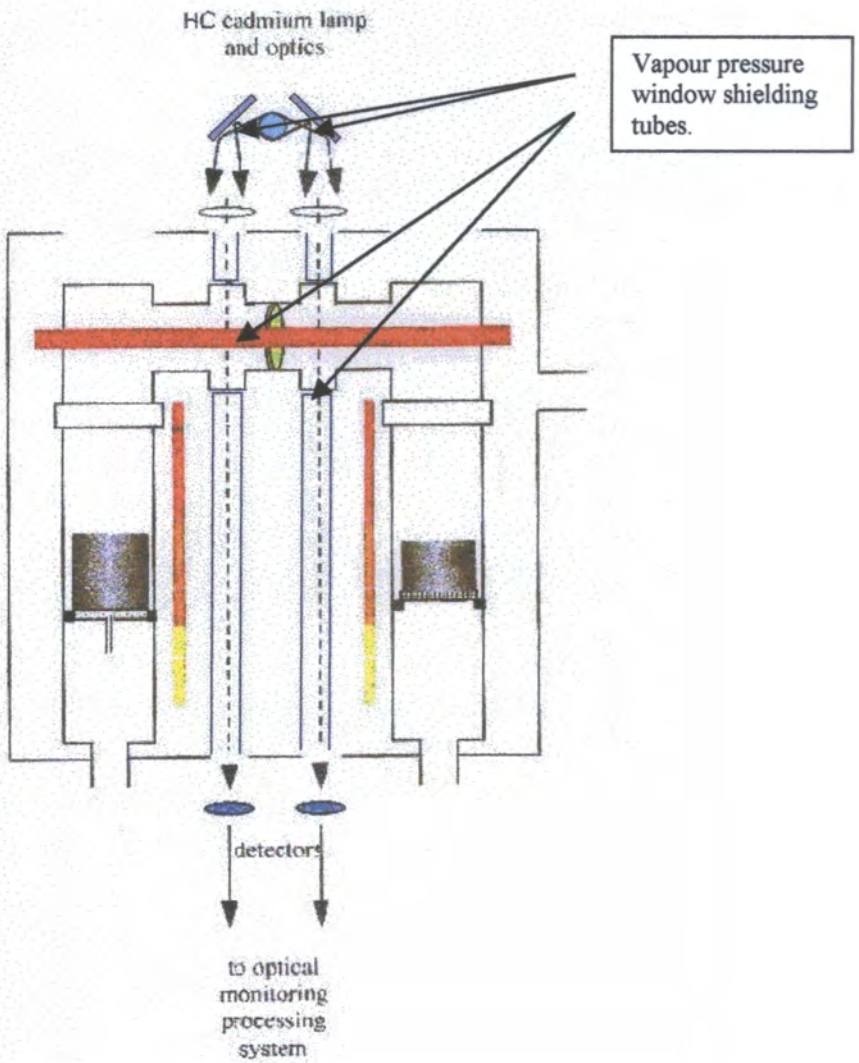

Fig 3.4, EDAX spectra of growth side vapour pressure monitoring window after run without shielding tubes

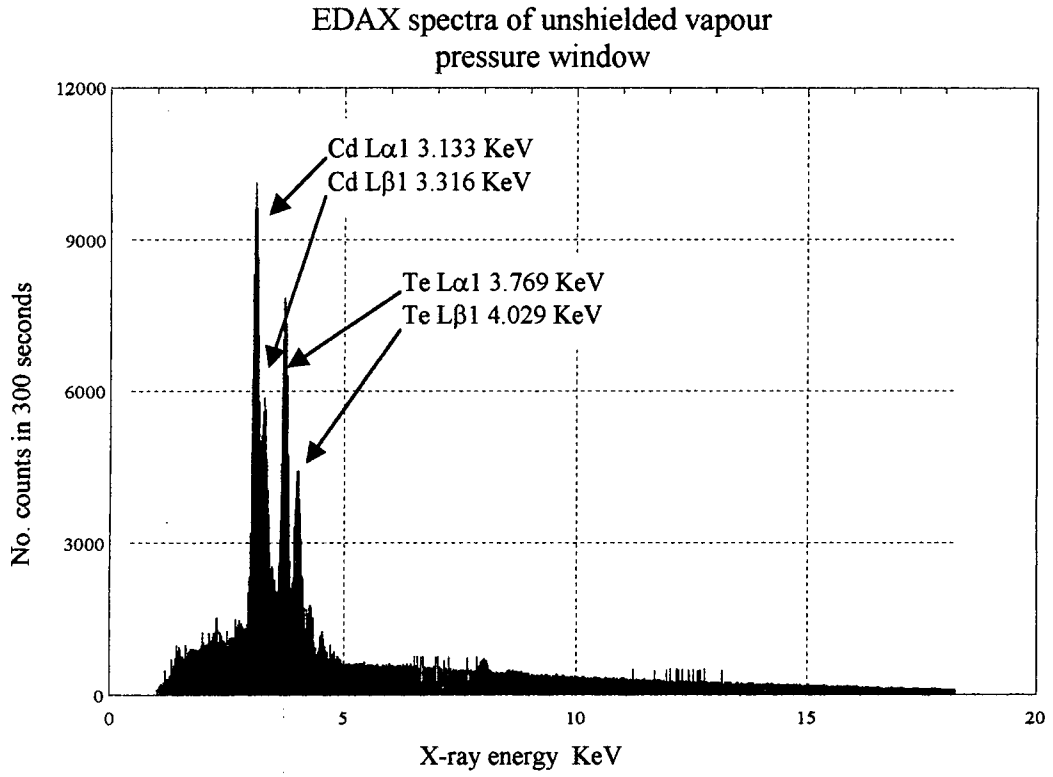

Fig 3.5, EDAX spectra of growth side vapour pressure monitoring window after run with cracked vapour pressure shielding tube

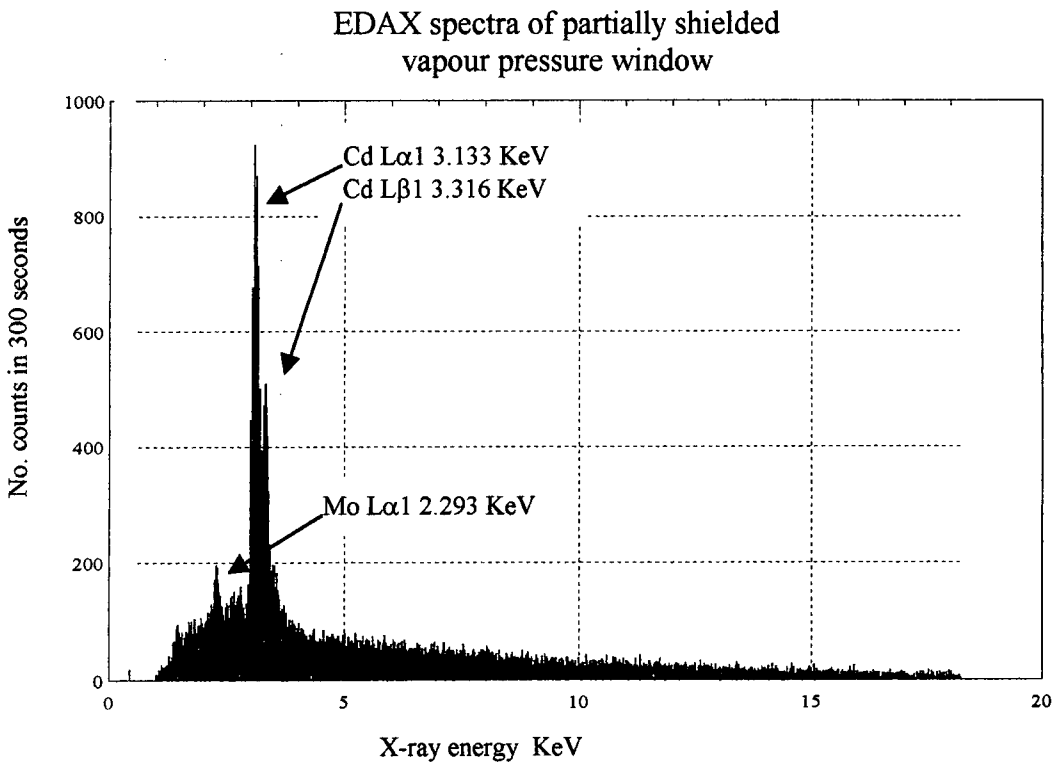

Fig 3.6, EDAX scan of source side vapour pressure monitoring window after growth run with shielding tubes in place.

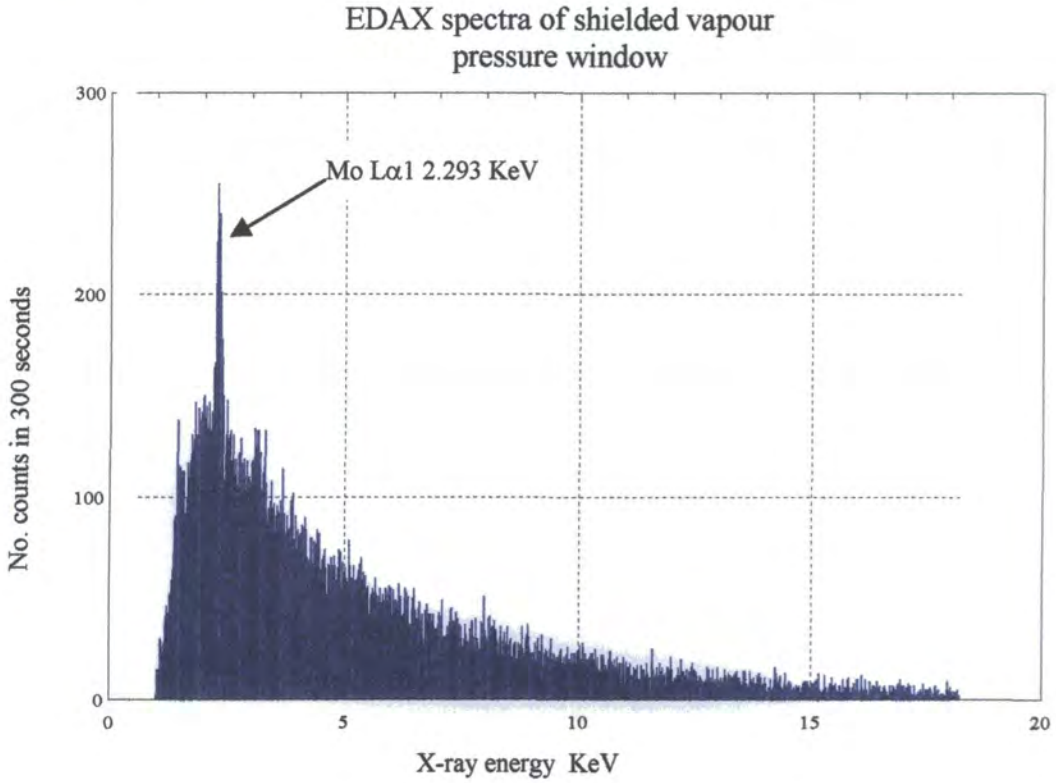

Fig 3.7, Transmission spectrum of vapour pressure monitoring windows after a growth run with and without shielding tubes in place.

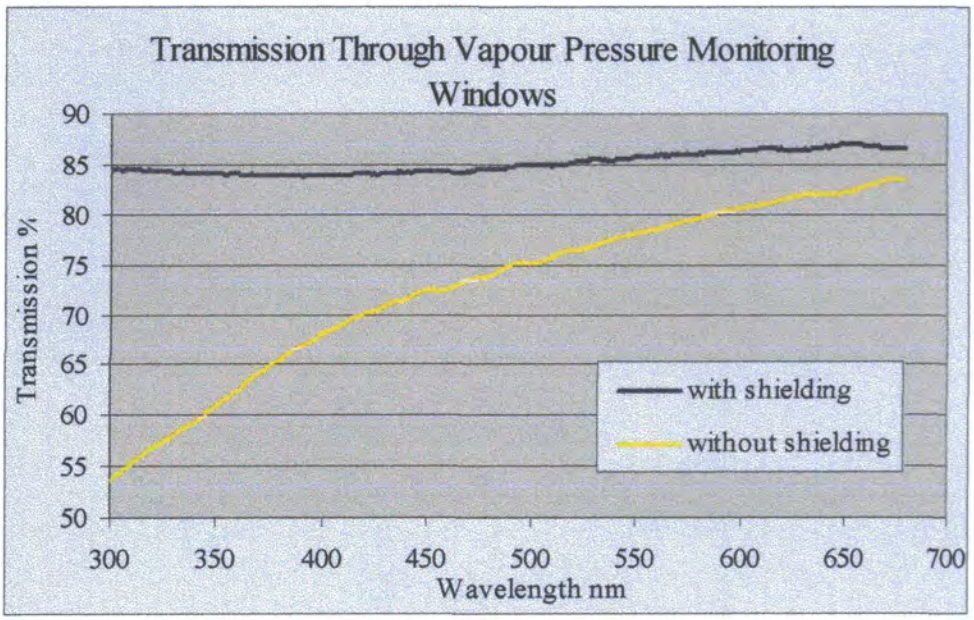

A substantial amount of material was deposited on the vapour pressure monitoring windows during growth runs performed without the shielding tubes in place, and EDAX analysis showed the dark, semi-transparent coating was cadmium and tellurium as shown in *fig (3.4)*.

On the occasion where one of the shielding tubes had been cracked, a silver semi-reflective deposit was observed to form during the growth run. EDAX analysis showed this to be only cadmium. Possible explanations for the absence of tellurium in the window deposit are the higher temperature of the window due to the radiative heating action of the crossmember, and the lower mobility and larger size of molecular tellurium compared with atomic cadmium, resulting in a greater flow rate of cadmium atoms through the ground glass joints of the growth ampoule, and also through the gap in the window shielding tube resulting in predominantly cadmium vapour being present near the windows.

During growth runs where the shielding tubes remained intact there were no traces of cadmium or tellurium deposits on the vapour pressure window as shown by the EDAX analysis displayed in *fig (3.6)*. The absence of cadmium and tellurium generated x-rays makes the presence of molybdenum more obvious, and some counts were recorded for the molybdenum Lα1 x-ray emission in *figs (3.4)*, *(3.5)*, and *(3.6)*. The sources of molybdenum inside the MTPVT system are the molybdenum heat shields located around the furnace tubes and molybdenum wire used to support thermocouples within the furnace tubes (see chapter 2).

The effect of cadmium telluride deposit on the transmission spectra of the windows is shown in *fig (3.7)* where transmission has been measured over the wavelength range significant to the vapour pressure monitoring system after runs with and without the shielding tubes in place. The shielded window transmission spectra is fairly uniform

as expected for clear quartz glass, where as the unshielded window shows an absorption behaviour relation with wavelength, consistent with the absorption of light by a semiconductor such as CdTe.

The window shielding tubes greatly reduced deposit on the vapour pressure monitoring windows by both providing a physical barrier and increasing the temperature of the windows by radiating heat from the crossmember. *fig (3.5)* suggests the physical barrier provided by the tubes is the dominating effect as material is still deposited on the window despite its higher temperature, and it would be advantageous to make the seal between the shielding tubes and the window as tightly as possible while still allowing them to be evacuated by the surrounding vacuum jacket.

References for chapter 3

1 A. W. Brinkman, J. Carles, The Growth of Crystals From The Vapour, Progress in Crystal Growth and Characterisation of Materials (1998) 169-209

2 A. S. Berman, Free Molecule Transmission Probabilities, J. App. Phys., 36, (1965) 3356

3 A. S. Berman, Free Molecule Flow in an Annulus, J. App. Phys., 40, (1969) 4991

Chapter 4

Synthesis of Cadmium Telluride Source Material

Chapter 4

Synthesis of Cadmium Telluride Source Material

4.1 Introduction

Semi-open growth is more tolerant of source material quality than closed ampoule growth as impurities and excess components will diffuse away from the growing surface via the annulus gap. This effect overcomes some of the difficulties caused by the non congruent sublimation of cadmium telluride (see chapter 1). Nevertheless, it is desirable to have source material as close as possible to stoichiometry and of the highest possible purity. The source is also required to be dense with a uniform evaporating surface. This chapter concerns the preparation of the CdTe source material used for vapour growth in the MTPVT system.

4.2 Method

4.2.1 Material Preparation

Ingots of 99.999% pure cadmium and tellurium were cut into lumps of approximately ½ cm^3. Tellurium, being a brittle metal, was easily broken into small pieces of the appropriate size without having to use cutting tools, or remove it from its protective polythene wrapping. The ductile nature of cadmium however meant a hydraulic press was needed to drive a stainless steel blade through the metal, with the possibility of contamination. Ideally, all preparation of the metals should be conducted in a glove

box, or a clean room, however these facilities were not available. Better still, the ingots should be pre-cut to the correct size so they could be transferred to the ampoule inside a glove box, without coming into contact with the outside world.

4.2.2 Ampoule Preparation

The ampoule was formed from 45 mm diameter, 40 cm length, quartz tube. Because of the chance of material becoming stuck to the glass and causing stress during the heating or cooling process, tubing was selected with 2 mm thick walls to reduce the chance of fracture during synthesis. The tube was sealed at one end, and the other end was tapered down to a 15 mm diameter tube. At this point, the ampoule was cleaned by washing with 40 % hydrofluoric acid, followed by a thorough rinse with de-ionised water. The ampoule was then baked out at 1000 °C under dynamic vacuum for 24 hours. The ampoule was filled to no more than a third full, again to reduce the chance of fracture, with the prepared cadmium and tellurium in the ratio of their atomic masses, i.e. 1 part by weight cadmium to 1.1351 parts by weight tellurium. The diameter of the ampoule entrance was then reduced from 15 mm to 7 mm diameter tube to make the sealing process more reliable. It was then evacuated and baked out at 200 °C under dynamic vacuum for a further 24 hours. Before sealing the ampoule it was back filled with 0.2 atm (so that at the synthesis temperature of 1100 °C the pressure inside the ampoule would be no more than 1 atmosphere) of high purity argon, to act as a heat conductor and ensure the metals melted uniformly. The ampoule was then sealed as quickly as possible.

4.2.3 Furnace Temperature Profile.

Temperature data from the source mid furnace zone, in the MTPVT system, which is used to take an estimate of the source vapour pressure and set to give specific transport rate, is only known precisely within a short range of the measuring thermocouple, without having to estimate temperatures using thermal modelling. It is therefore desirable to have the source material in a well defined position, and in as narrow a temperature range as possible. For this reason, the source material must be compacted during the synthesis process. If the synthesis ampoule was held at a uniform temperature, then the newly formed cadmium telluride would condense throughout the ampoule, it is therefore necessary to pull the ampoule along a temperature gradient to condense the material at the coolest point. This was achieved by slowly pulling the ampoule through the vertical temperature gradient of a furnace (see *fig 4.1*), while maintaining the temperature of the reacting mixture at 1100 °C by locating the controlling thermocouple on the ampoule.

The ampoule was heated to 250 °C at a rate of 10 °C per minute, and then to 350 °C at a rate of 1 °C per minute. The temperature was maintained at 350 °C for 60 minutes, during which the cadmium began to melt and the reaction between cadmium and tellurium started. As this is an exothermal reaction, the temperature was allowed to stabilise in case a rapid temperature increase caused the ampoule to fracture.

After 1 hour, the temperature was increased to 1100 °C at a rate of 1 °C per minute.

To begin the compacting process, after 2 hours at 1100 °C the ampoule was pulled at a rate of 0.8 cm per hour for 24 hours, at which point the reaction was considered to be complete, the pulling was stopped and the ampoule cooled to room temperature at a rate of 1 °C per minute. It is during the cooling process that the largest potential

stresses can occur, due to the effect of differential thermal expansion, particularly for cadmium telluride that has adhered to the quartz glass, it is again important therefor to change the temperature as slowly as possible.

fig 4.1 Cross section of furnace and ampoule.

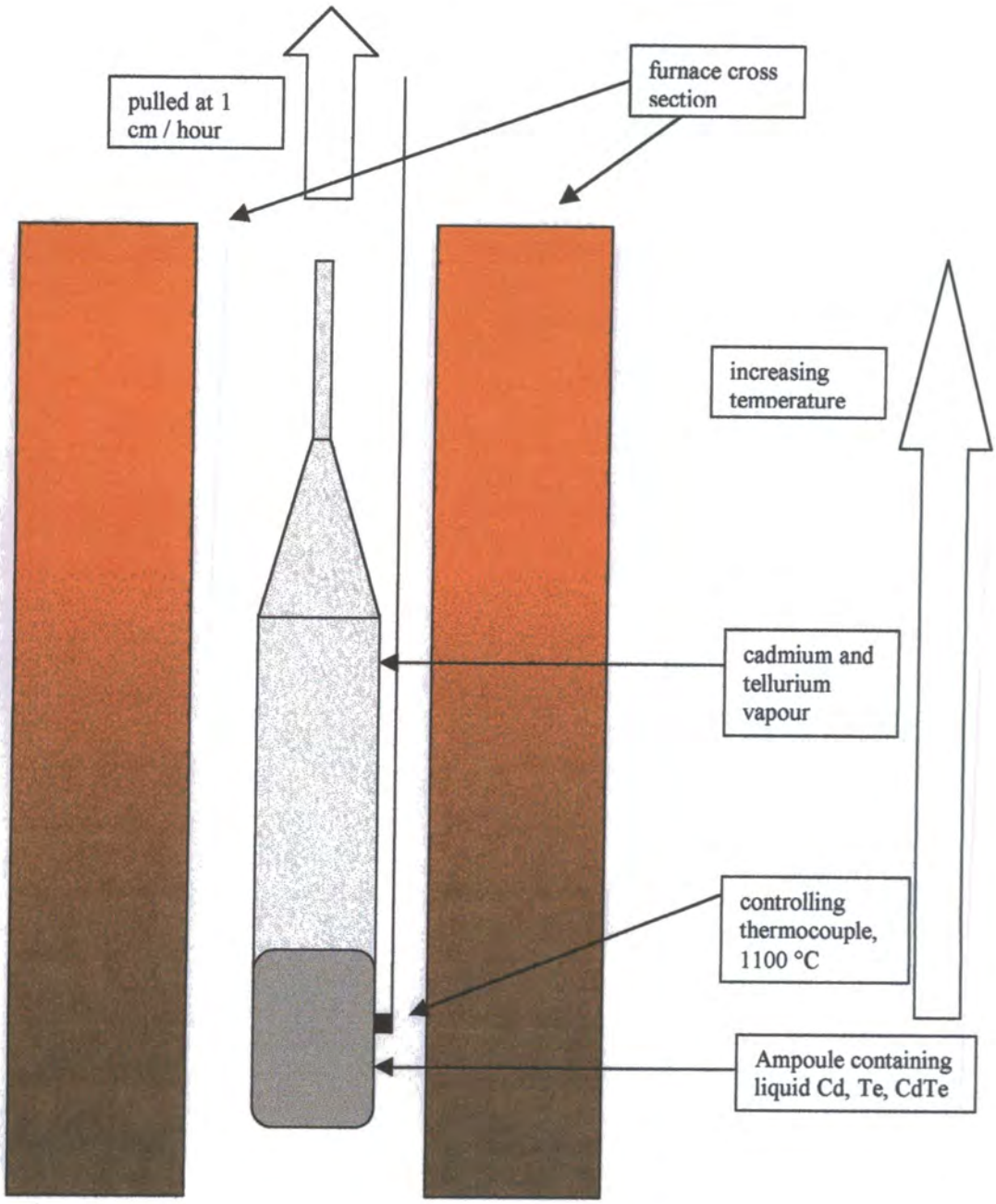

4.3 Conclusion.

A boule of polycrystalline cadmium telluride was synthesised from 136.452 gms of cadmium and 154.889 gms of tellurium. The 291 grams of material was compacted to fill approximately 5 cm of the 25 cm long ampoule. The purity and stoichiometry of the cadmium telluride source material could not be assessed as this would involve opening the ampoule and taking a sample, thereby compromising the purity of the source.

The outside of the synthesis ampoule was thoroughly cleaned with acetone followed by deionised water before being opened at atmospheric pressure and inserted into the growth ampoule immediately before pump down. The cadmium telluride source material was used in growth run 44 (see chapter 6).

Chapter 5

Calibration of the Crossmember Flow Restrictor

Chapter 5

Calibration of the Crossmember Flow Restrictor

5.1 Introduction

For the growth from the vapour phase of bulk CdTe crystals which are uniform in structure, stoichiometric in composition and free from voids, inclusions or precipitates, then, as described in chapter 1, a constant vapour pressure ratio above source and growing crystal is essential if fluctuation free growth is to be attained. As CdTe does not necessarily sublime stoichiometrically due to uncertainty in the composition of the starting material, (due to a high abundance of the many isotopes of cadmium present in nature) in a closed system diffusion barriers would be set up at the crystal surface which would be both growth rate limiting and could cause the formation of inclusions or precipitates(*ref 1, 2, 3*), especially if there were significant foreign species in the source material. In the semi-open, Markov type system, any excess components or impurities can diffuse away from the growing area, but only up to a certain rate. If transport rates are too high then the excess impurities will not have time to reach an equilibrium point, and any impurities may not be removed fast enough. It is therefore necessary to control the rate of mass transfer, as realised by Rosenberger et al (*ref 4*), whose calculations showed that for typical ampoule dimensions and vapour pressures during growth, transport rates would be too high for crystals with good morphological and structural properties to be grown.

It is necessary to have some degree of control over vapour pressure ratio and mass transport rate in order to fully study the mechanisms of mass transport and growth,

and attain reproducible results. There is also the question of maximising growth rate and material utilisation efficiency from a commercial point of view.

Some sort of mass transport restrictor between source and growth is necessary, allowing source material and growing crystal to be thermally decoupled. This allows the seed to be maintained at a stoichiometrically favourable temperature, while the temperature of the source material can be adjusted to provide a mass transport rate low enough to allow excess components time to diffuse away, and Cd and Te atoms time to be incorporated into the growing lattice uniformly, but high enough to be commercially viable.

The initial choice for restrictor was a porous silica sinter disc, however this proved to be too restrictive, and any replacement would have to be calibrated. The second choice was a short section quartz of capillary tube. A capillary was chosen as the fluid mechanics are well understood, and they are easily reproduced and readily available in a variety of dimensions.

5.2 The Fluid Dynamics of Capillary Flow

There are several mechanisms by which fluids can pass through capillary tubes. Most importantly in this context the flow can be molecular, viscous or a combination of the two depending on the mean free path of the gas and the diameter of the capillary, or more specifically the ratio or the two. The flow can also be laminar, turbulent, or a combination of the two depending on the pressure drop across the capillary, physical influences such as entry and exit flow from the capillary, and capillary length. Thirdly, the flow can be compressible depending on the ratio of entry and exit pressure of the capillary.

Clearly it is necessary to calibrate mass transport rate with respect to pressure drop across the capillary, understand the mechanisms behind this relation, and use this knowledge to extrapolate the relationship to growth conditions and species. Knowledge of the flow mechanisms in the capillary is essential as these influence mass transport of the elements and growth rate, it also allows the selection of particular growth parameters for study. For experimental ease and safety, flow calibration was conducted out of the system at room temperature using inert gasses.

5.3 Molecular Flow.

Molecular, or Knudsen flow occurs when the mean free path of the molecules, λ, is appreciably greater than the radius of the capillary r. Therefore collisions between the gas molecules and the capillary walls dominate over collisions between the molecules themselves (*ref 5*).

The Knudsen flow of a gas with molecular weight M, through a capillary of radius r and length L is given by *eq 5.1* where R is the universal gas constant, T is the absolute temperature and ΔP is the pressure difference between the ends of the capillary (*ref 5*).

$$F_K\left[\frac{moles}{t}\right] = \frac{2\pi r^3}{3}\left(\frac{8RT}{\pi M}\right)^{1/2}\frac{\Delta P}{LRT} \qquad eq\ 5.1$$

This is only true for $\lambda >> r$ and $L >> r$.

5.4 Viscous Flow

Viscous flow through a capillary occurs when collisions between molecules dominate transport and collisions with the walls can be neglected. Viscous flow is given by Poiseuille's equation, *eq 5.2*. This applies where the gas is incompressible, the flow is laminar, the flow velocity is zero at the capillary walls and the mean free path of the molecules is much less than radius of the tube ($\lambda << r$). Usually for fully developed laminar flow it is required that $L >> r$ as turbulence is caused at the entry to and exit from the capillary.

$$F_V\left[\frac{moles}{t}\right] = \frac{\pi r^4 P_m \Delta P}{8\eta LRT} \qquad eq\ 5.2$$

where η = fluid viscosity and P_m = mean pressure across the capillary, (*ref 5*)

5.5 Mixed Flow

When the mean free path $\lambda \sim r$ then a transition region occurs where the flow is not entirely molecular or viscous. In this regime there is no absolute expression for flow rate. An approximation is made by using the Poiseuille formula with a correction term derived qualitatively from the assumption that flow rate at the walls is now non zero *eq 5.3*, (*ref 5,6*)

$$F_M\left[\frac{moles}{t}\right] = \frac{\pi r^4 P_m \Delta P}{8\eta LRT} + \frac{\pi^2 r^3 \Delta P}{(8\pi MRT)^{1/2} L}\left(\frac{2}{f} - 1\right) \qquad eq\ 5.3$$

The friction factor, f is a measure of the fraction of gas molecules diffusely reflected from the capillary walls and is given by *eq 5.4.*

$$f = \frac{\tau_\omega}{0.5\rho v^2} \qquad \text{eq 5.4}$$

Where τ_ω = shear stress between molecules and capillary walls, ρ = density of gas and v = flow velocity,(*ref 7*).

The Knudsen number gives some idea of the type of flow to be expected. It is defined as $K_d = \lambda/r$ and as a guide it can be taken that :-

Molecular flow	$K_d > 3$
Viscous flow	$K_d < 0.01$
Transition flow	$3 > K_d > 0.01$

(*ref 8*)

5.6 Compressible and Turbulent Flow

As the pressure drops through the capillary, so the gas expands according to the universal gas law. This gives rise to compression effects which affect mass transport (*ref 9*). The mach number of the fluid provides a measure of compression effects. Mach number is defined as the ratio of the velocity of the gas to the speed of sound in the gas, i.e. $M = V/c$. This can also be written in terms of the ratio of specific heat at constant volume to specific heat at constant pressure, γ, which is 1.4 for a perfect gas, *eq 5.5.*

$$M^2 = \frac{V^2}{\gamma RT} \qquad \textit{eq 5.5}$$

As the density of a particular gas reduces through a capillary tube with pressure drop, so the speed of sound in the gas reduces. If a point is reached where the speed of sound at the capillary exit is less than the entry velocity of the gas then it will no longer be possible for information about the downstream gas, in the form of a shock wave, to be passed upstream, resulting in flow saturation. The flow rate will tend towards saturation as the mach number of the gas at the capillary exit tends to 1. Typical mach numbers under growth conditions range between 0.4 and 0.6, (during run 44 the average vapour velocity through the flow restrictor was 130 ms^{-1} with the speed of sound being 240 ms^{-1}(see sec 6.3.1)). Typical Knudsen numbers encountered during growth vary between 0.5 and 1, meaning flow is transitional and the effects of compression reduced as this is a purely viscous flow effect (see sec 5.5). For this reason compression effects are ignored during growth.

At growth and calibration conditions the Reynolds number, *Re*, which indicates whether the flow will be turbulent, laminar, or some intermediate stage, is too small for turbulence to be develop to any significant extent. There will always be some degree of turbulence at the entry point, it has been shown that viscous flow develops after a certain distance down the tube, (*ref 10*). which is given by the expression $l_d = 0.227rRe$. Hence for typical Reynolds numbers encountered during calibration and under growth conditions, (<200), it can be assumed that viscous flow is fully developed before the end of the capillary.

5.7 Room Temperature and Growth Temperature Conditions.

Calibration was conducted at room temperature, 290 K, using the gases nitrogen, helium, argon and sulphur hexafluride. Typical pressure drops across the capillary

varied between 0.2 mbar and 35 mbar. More importantly the pressure ratio, the ratio of inlet pressure to outlet pressure, varied between about 1.2 and 4. This is important as it is the pressure ratio which determines the compression of the gas through the tube at a given temperature and flow rate.

At growth conditions the temperature is of the order of 1170 K ± 50 K and typical pressure drops are of the order 5 mbar with pressure ratios of about 2.

5.8 Experimental Set-up

Fig 5.1 Schematic diagram of crossmember calibration arrangement

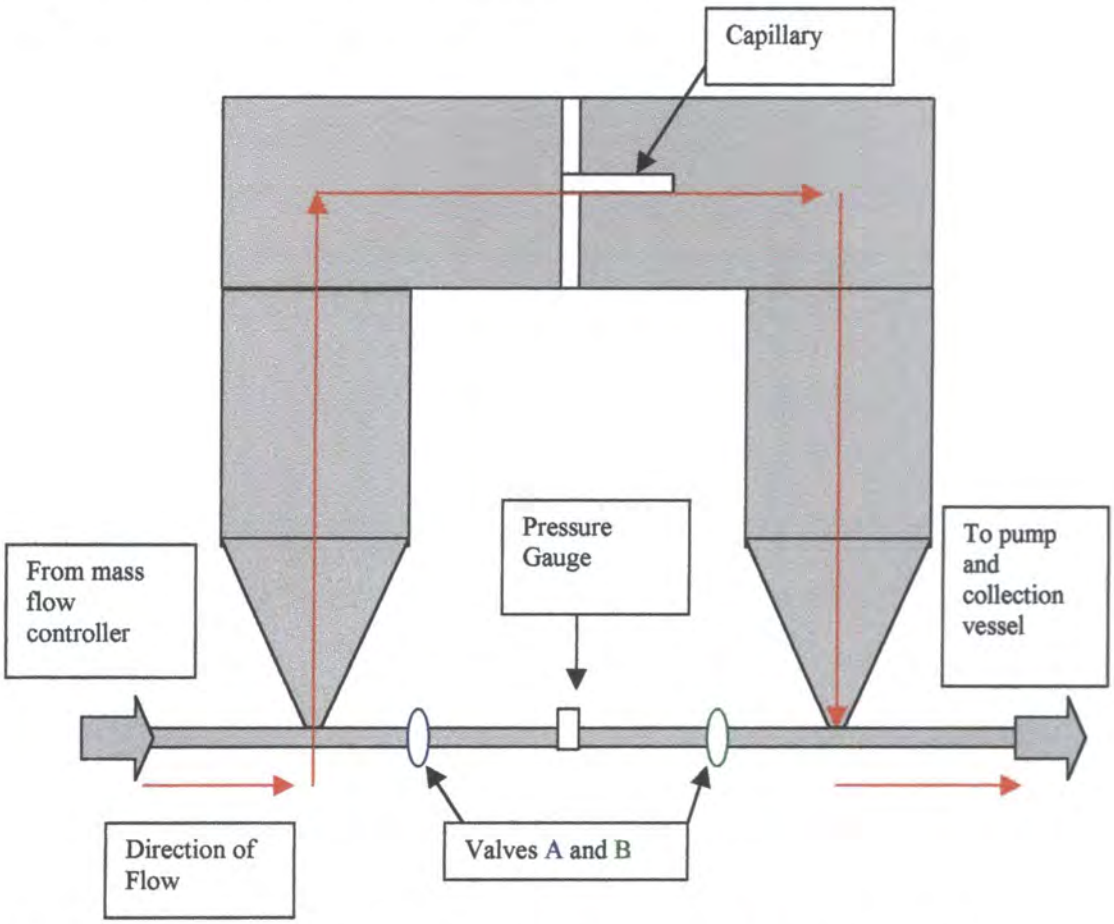

For calibration of the capillary flow restrictor, both ground glass joints of the crossmember were connected to specially made ground glass connectors which joined to 7mm diameter vacuum pipe, see *fig(5.1)*.

A mass flow controller was used to govern molar flow rate (Brooks Mass Flow

Controller 5850TR). Pressure was measured using a Druck pressure indicator. Valves A and B allowed pressure to be measured on either side of the capillary. A rotary pump was used to pump the system and gas was collected over water at standard temperature and pressure via the pump exhaust. The test gases He, N_2, Ar and SF_6 were used for calibration. Measurements were made of the A and B side pressures for different molar flow rates. The mass flow controller was operated by setting a voltage which was proportional to the mass flow. For each gas the mass flow controller was calibrated by measuring the volumetric flow rate at standard temperature and pressure for several voltages across it's range. Experimental measurements were therefore the A and B side pressures for each mass flow control voltage selected. Care was taken to ensure equilibrium had been reached after each flow rate was selected.

5.9 Results

The volumetric flow rate (in standard cubic centimetres per second) and the respective pressures on each side of the capillary (in mbar) for each gas tested can be found in Appendix1.

The specific flow rate (moles sec^{-1} ΔP^{-1}) was then plotted against the mean pressure across the capillary (P_m) (*fig 5.1 through 5.4*). As can be seen from *eq 5.3*, for mixed viscous and molecular flow, such a plot should yield a straight line with gradient proportional to the viscosity of the gas and intercept proportional to the friction factor. Deviation from this condition is due to compression saturation of the flow.

Fig 5.1 Specific flow rate vs mean pressure for helium

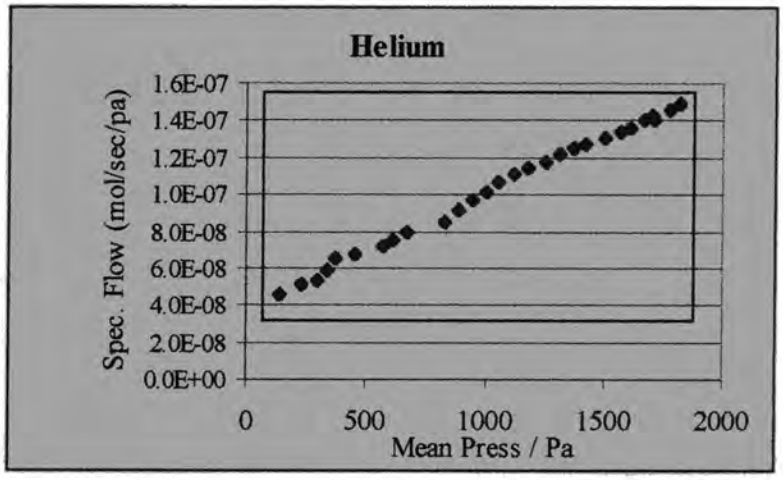

Fig 5.2 Specific flow rate vs mean pressure for nitrogen

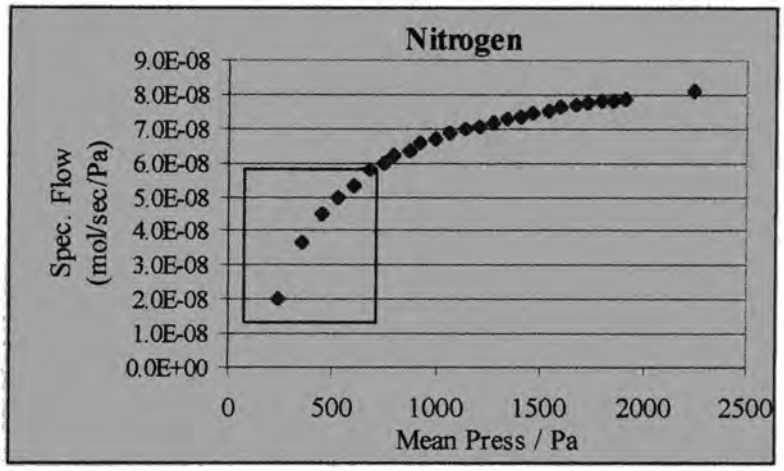

Fig 5.3 Specific flow rate vs mean pressure for argon

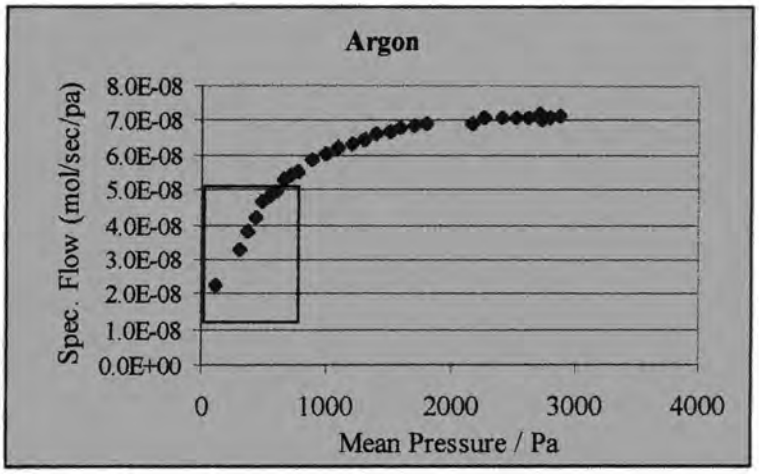

Fig 5.4 Specific flow rate vs mean pressure for SF_6

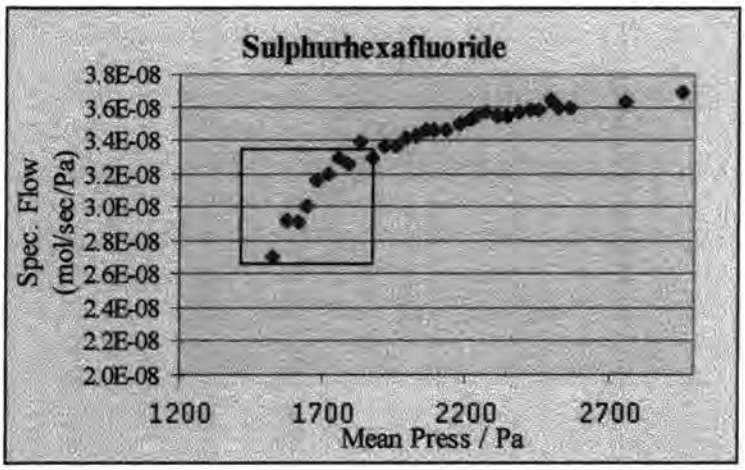

The highlighted sections were fitted to equation *5.3* for each gas.

5.10 Capillary Dimensions

Flow through the capillary varies as r^4 for viscous flow, and r^3 for molecular flow so an accurate value for the capillary radius is needed. By measuring the mass of mercury which filled the capillary a more precise value of average radius was found than that which could be measured using a travelling microscope. The capillary radius was found to be $r = 0.519 \pm 0.002$ mm.

5.11 Discussion and Conclusion

As can be seen from figs *5.2, 5.3* and *5.4*, gas flow through the capillary is saturated and further increases in specific flow with pressure difference were not possible. This appeared not to be the case for helium flow *fig (5.1)*. The speed of sound in helium is much higher than that for the other gases, due to the much smaller molecular mass. Therefor under the same calibration conditions, compression effects are less

pronounced, although under close inspection *fig (5.1)* shows a slight trend towards saturation.

Taking the straight line sections of the graphs and fitting a linear equation allowed calculation of viscosity and friction factor from the slope and intercept of the fitted line using *eq 5.3.*

Rearrangement of *eq 5.3* gives,

$$\text{Slope (m)} = \frac{\pi r^4}{8\eta LRT} \qquad \textit{eq 5.6}$$

$$\text{Intercept (c)} = \frac{\pi^2 r^3}{(8\pi MRT)^{1/2} L}\left[\frac{2}{f} - 1\right] \qquad \textit{eq 5.7}$$

Where T is 290 K.

Table 5.2 Intercept and slope of eq 5.3 when fitted to calibration data from test gases

	N_2	Ar	He	SF_6
molecular weight	2.80E+01	3.99E+01	4.00E+00	1.46E+02
slope, m	5.75E-11	6.05E-11	6.17E-11	2.50E-11
intercept, c	1.83E-08	1.54E-08	3.81E-08	1.09E-08
viscosity (Pa.S)	1.77E-05	1.68E-05	1.65E-05	4.07E-05
fction factor	9.89E-03	9.85E-03	1.26E-02	7.30E-03

Table 5.2 contains the slopes and intercepts calculated for each gas as well as the friction factor and viscosity in SI units as calculated from *eq 5.6* and *eq 5.7.*

It was shown in the work by J. C Alabert, (*ref 11*), that friction factor is constant with molecular mass and temperature, over the range of temperatures and molecular mass relevant to growth and calibration conditions. This was found for a much more restrictive porous sinter disc. Plotting the above intercepts against $1/\sqrt{M}$ confirms this result for the capillary tube used here (*fig 5.5*) as the intercept is proportional to $1/f$ for

constant r, L and T (see *eq 5.7*).

fig 5.5 Plot of intercept (from eq.5.7) against $\sqrt{M}$ *for each test gas.*

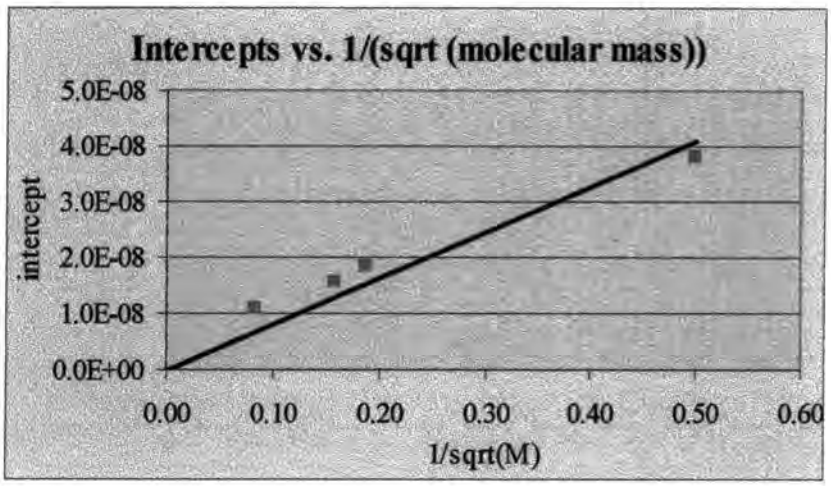

It is now necessary to extrapolate these results to growth conditions. Temperatures range from 1120 K to 1220 K and the molecular masses of cadmium and tellurium are 112.41 and 255.20 respectively. Taking the mean friction factor, as calculated from the slope of *fig (5.5)*, and using van der Waals rigid sphere model to calculate the approximate viscosity of cadmium and tellurium over the temperature range of interest, specific flow can be calculated knowing the A and B side pressures.

$$\eta = \frac{2.67\times10^{-20}(MT)^{1/2}}{d^2} \quad Pa.S \qquad\qquad eq\ 5.8$$

where d is the molecular diameter of Cd or Te_2. (This calculation will give an inaccurate result for the viscosity of tellurium as it is a molecular gas and is therefor not well represented by a rigid sphere model, in later analysis however, only Cd atoms will be considered).

Inserting values for η (9.00×10^{-5} Pa.S), r (5.19×10^{-4} m), L (1.17×10^{-2} m), M (112.41)

and $f(1.176\times10^{-2})$ into *eq 5.3*, the specific flow of cadmium through the crossmember capillary is therefore given by *eq 5.9*.

$$F_M\left[\frac{moles}{t}\right] = 3.28\times10^{-9}\frac{P_m\Delta P}{T} + 1.31\times10^{-7}\frac{\Delta P}{\sqrt{T}} \qquad eq\ 5.9$$

In principle *eq 5.9* should allow the selection of a source temperature and pressure which will give a transport rate favourable for the growth temperature chosen for study.

The uncertainty in the calculation will be of the order of 10 %, considering the approximations made in the calculation of viscosity, and the non ideal flow conditions in the capillary. Empirical confirmation and correction of *eq 5.9* during growth will be required before the precision of the model is known, necessitating systematic study of the system under a wide variety of growth conditions.

References for chapter 5

1 M. M. Faktor, R. Heckingbottom, I. Garret, Growth of Crystals form the Gas Phase part 1. Diffusional Limitations and Interfacial Stability in Crystal Growth by Dissociative Sublimation, J. Chem. Soc A (1970) 1257

2 M. M. Faktor, R. Heckingbottom and I. Garret, Growth of Crystals form the Gas Phase part 2. Diffusional Limitations and Interfacial Stability in Crystal Growth by Dissociative Sublimation, with an Inert Third Gas Present, J. Chem. Soc A, (1971) 1

3 M. M. Faktor, R. Heckingbottom and I. Garret, Diffusional Limitations in Gas Phase Growth of Crystals, J. Crystal Growth, 9 (1971) 3

4 F. Rosenberger, M. Banish and M. B. Duval, Vapour Crystal Growth Technology Development- Application to Cadmium Telluride, NASSA Technical Memorandum 103786 (1991)

5 R. D. Present, Kinetic Theory of Gases, McGraw-Hill, New York (1958)

6 W. G. Pollard and R. D. Present, Gaseous Self Diffusion in Long Capillary Tubes, Phys. Rev., 73 (1948) 762

7 G. P. Brown, A. DiNardo, G. K. Cheng, T. K. Sherwood, The Flow of Gases in Pipes at Low Pressures, J. Appl. Phys., 17 (1946) 802

8 L. Holland, W. Steckelmacher, J. Yarwood, Vacuum Manual, E. & F. N. Spon, London (1974)

9 M. A. Saad, Compressible Fluid Flow, pub Englewood Cliffs, (1993)

10 S. Dushman, J. M. Lafferty, Scientific Foundations of Vacuum Technique, 2nd edition, John Wiley & Sons, New York (1962)

11 J. C. Alabert, Optical Vapour Pressure Monitoring and Mass Transport Control During Bulk CdTe Crystal Growth in a Novel Multi Tube PVT System, Appendix A, Ph.d. Thesis University of Durham, UK, (1998)

Chapter 6

Mass Transport in the MTPVT System

Chapter 6

Mass Transport in the MTPVT System

6.1 Introduction.

The mass transport rate of Cd and Te vapour to the growing crystal under different growth conditions must to be known if any detailed analysis of the effect of transport rate on crystal properties is to be possible. The arrival rate of Cd atoms and Te_2 molecules for any given growth interface temperature is important if the species are to be able to join the crystal lattice at a rate which is allowed by the kinetics of the growing surface, i.e. if transport rate is too high then Cd and Te atoms will not arrange themselves in the lattice in a uniform manor and crystal quality will be reduced. A transport rate that is too low however would, from a commercial point of view, result in a reduction in production efficiency.

In this chapter the mass of CdTe transported from the source charge to growing crystal through the crossmember capillary, including material which has been lost past the annulus gap around the crystal holder, will be investigated over three separate growth runs of the MTPVT system. The measured mass transport will be compared with the theoretically predicted value, which will be calculated by integrating *eq 5.3* over the duration of each run. A reasonable correlation between predicted and measured mass transport for growth runs conducted under various conditions should, in principle allow the selection of a kinematically favourable transport and growth rate for a given growth temperature.

6.2 Theory.

The flow rate in moles per second through the crossmember capillary flow restrictor was discussed in section 5.5 and is given by: -

$$F_M\left[\frac{moles}{t}\right]=\frac{\pi r^4 P_m \Delta P}{8\eta LRT}+\frac{\pi^2 r^3 \Delta P}{(8\pi MRT)^{1/2} L}\left(\frac{2}{f}-1\right) \qquad eq\ 5.3$$

(*ref 1,2*) where ΔP = pressure difference across the capillary, P_m is the mean pressure across the capillary, T is the absolute temperature of the capillary, f is the friction factor (see section 5.5), L and r are the capillary length and radius respectively, R is the universal gas constant, η is the viscosity of cadmium vapour and M is the molecular mass of cadmium.

Equation *5.3* can be expressed in terms of source and growth side pressures, P_s and P_g respectively, by letting:-

$$\Delta P = P_s - P_g$$

$$P_m = (P_s + P_g)/2$$

For simplicity let $\frac{\pi r^4}{8\eta LR} = K_v$ and $\frac{\pi^2 r^3}{\sqrt{(8\pi MR)}L}\left[\frac{2}{f}-1\right] = K_m$

Expanding *eq 5.3* then gives the mixed viscous and molecular component flow rate, F_M as:-

$$F_M\left[\frac{mol}{t}\right]=\frac{K_v P_s^2}{T_c}+\frac{K_m P_s}{\sqrt{T_c}}-\frac{K_v P_g^2}{T_c}-\frac{K_m P_g}{\sqrt{T_c}} \qquad eq\ 6.1$$

where T_c is the temperature of the crossmember.

The number of moles of cadmium vapour transported in a time t_{max} is therefore given by:-

$$F_M[mol]=\int_0^{t_{max}}\left[\frac{K_v P_s^2}{T_c}+\frac{K_m P_s}{\sqrt{T_c}}-\frac{K_v P_g^2}{T_c}-\frac{K_m P_g}{\sqrt{T_c}}\right]dt \qquad eq\ 6.2$$

The vapour pressure of cadmium over cadmium telluride in the temperature region encountered during vapour growth is given by the equation (*ref 3*).

$$P_{Cd} = 1.26\left[\exp-\left\{\frac{6.9446\times10^4 - 45.842T}{1.9872T}\right\}\right]^{2/3} \qquad eq\ 6.3$$

where P_{cd} is the pressure of cadmium in atmospheres and T is the absolute temperature of the cadmium telluride source charge, or the temperature of the crystal vapour interface. This expression gives the *equilibrium* cadmium partial pressure above cadmium telluride, however in semi-open vapour growth the conditions are not at equilibrium, it is therefore an approximation to take the equilibrium partial pressure. Given that data from the optical absorption vapour pressure monitoring system is not yet accurate to within a factor of 2, values of P_{Cd} as calculated from *eq 6.3* are the most accurate available.

As the boule of cadmium telluride grows vertically up the growth tube, so the temperature of the crystal vapour interface increases with time. By making the assumptions that the vertical temperature gradient is linear between the crystal holder and the top of the source tube (see *fig 2.1*), and that the height of the crystal increases linearly with time during growth, then the temperature of the growing surface can be calculated as it increases with height during a growth run. It was assumed that:-

$$T_g = p + qt \qquad eq\ 6.4$$

where T_g = temperature of growth interface, p = starting temperature, t = time from start of growth and $q = \dfrac{T_{g\max} - p}{t_{\max}}$.

T_{gmax} is the maximum temperature reached by the crystal vapour interface at a time t_{max} when the system cool down begins. T_{gmax} was estimated by measuring the height of the respective boule and calculating the temperature of the point of the same height

between the crystal holder (and the growth mid thermocouple) and the thermocouple at the top of the source zone.

The expression for T_g as given by *eq 6.4* was substituted back into *eq 6.3* to give a valid expression for growth side pressure, which was in turn substituted into *eq 6.1* to give a time dependent transport rate, allowing for the temperature increase of the growing surface.

A spreadsheet was used to perform the integration in *eq 6.2*. Growth pressure and flow rate was evaluated at 10 second intervals once the MTPVT had reached its set point temperature. The amount of cadmium transported in each 10 second interval was then summed over the growth period.

The amount of material transported during the heating up and cooling down process was calculated by assuming the growing surface was at a fixed position some fraction up the linear temperature gradient of the growth tube. The pressures P_g and P_s were then calculated from *eq 6.3* using the temperature data logged during the respective growth run. Knowing the time interval between each temperature measurement the integral of *eq 6.2* can be summed as above except values of P_s and T_c are no longer constant. The spreadsheet formulae are given in *appendix 2*.

6.3 Results and Discussion.

Three separate growth runs of the MTPVT system were selected for study (run 44, 41, and 45). The temperature profiles of the significant heating zones (source bottom, source mid, growth mid, growth top and crossmember; see *fig (2.1)*) along with respective details and observations, are shown below for each run.

6.3.1 Run 44

Run 44 was conducted using the second of the growth tube arrangements, (see *sec 2.5*). *Fig (6.1)* shows the heating profile of the run. There were complications caused by the malfunction of one of the Pt/Pt13%Rh thermocouples, specifically the bottom source zone. The consequence of this was overheating of the bottom source zone, as can be seen from the red series in *fig (6.1)*. It was assumed that the vapour pressure of the source material was set by the hottest point of the source and the value of P_s in *eq 6.2* was accordingly set to the average temperature of the source bottom zone instead of the source middle zone.

fig 6.1 Temperature profile of run 44 of the MTPVT system

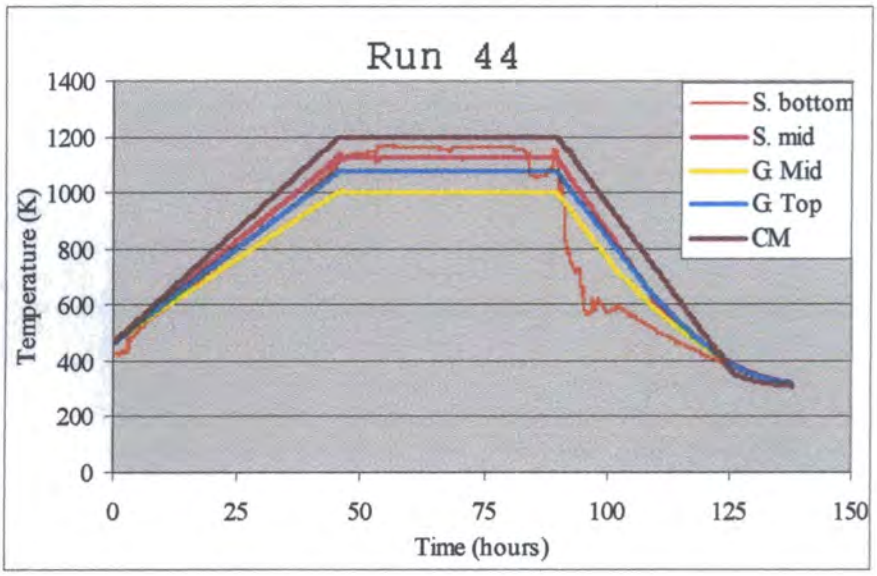

After 48 hours bakeout at 473 K, the temperature was ramped to growth conditions over 46 hours. After 44 hours at growth temperature, the temperature was reduced in a staggered ramp, the crossmember being cooled at the slowest rate to prevent condensation on the viewing windows.

The quartz plug, which supports the seed in the second growth tube arrangement, was separated from the walls of the ampoule by hardened platinum wire (see *sec. 2.5*). The

diameter of the wire chosen was 50 μm ± 5 μm. The uncertainty in the diameter of the platinum wire spacer, coupled with the grain size of the two ground glass surfaces which the wire separates (~10 μm) leads to an uncertainty of ~20% in the size of the gap between the crystal and ampoule wall.

The annulus gap around the crystal became blocked with cadmium telluride soon after growth temperature had been reached, this could be observed through the growth side viewing window (see *fig 6.2*). Possible causes of this could have been the unintentionally high transport rate caused by the excess source temperature, or the over restriction of the annulus gap.

fig 6.2

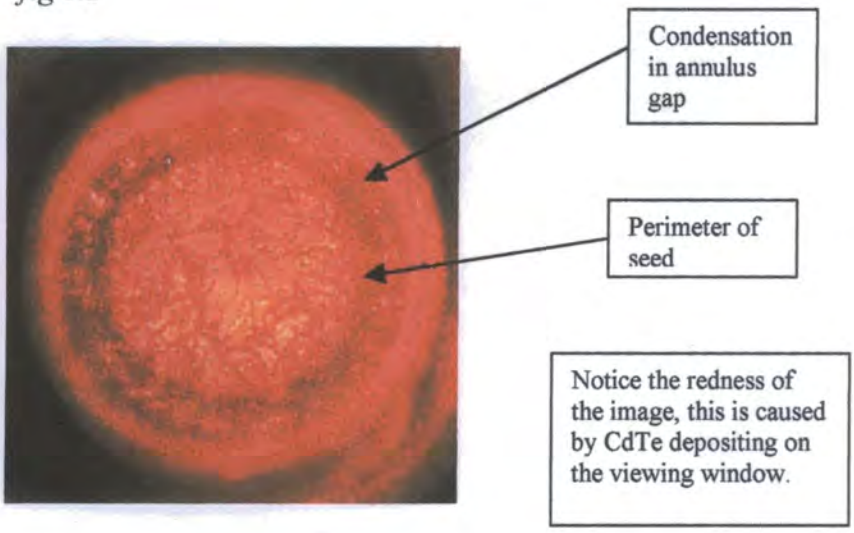

The total mass of cadmium telluride sublimed from the source side of the growth ampoule was 206.1 grams. The total mass of cadmium telluride to condense in the growth side of the ampoule was 204.7 grams. This represents a 0.7 % loss, far lower than the 5-10 % loss expected for semi-open vapour growth. This was attributed to the condensation of cadmium telluride in the annulus gap.

Assuming all of the 206.1 grams of material to leave the source side of the ampoule was transported through the crossmember flow restrictor, 0.8587 moles of cadmium were transported.

The number of moles of cadmium transported from source charge through the capillary flow restrictor to growing crystal, predicted from the capillary flow calibration of chapter 5 and *eq 6.3*, for the temperature profile shown in *fig (6.1)*, was 1.149 moles. This compares with the actual weighed transport of 0.8587 moles, representing a 25 % discrepancy.

Samples of the spreadsheet data used for the evaluation of *eq 6.2* are given in *Appendix 2.*

Figs (6.3), *(6.4)*, and *(6.5)* are plots of the spreadsheet data sampled in *Appendix 2.*

Fig 6.3

Plot of the mass flow rate during temperature increase calculated directly from thermocouple data. The trend of the plot is exponential as expected for a linear temperature increase, the noisy graph is due to small temperature variations.

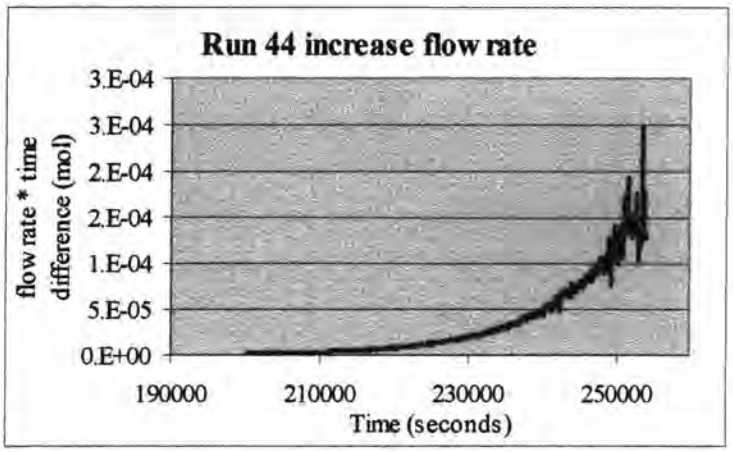

Area under increase flow rate plot =0.03125 moles

Fig 6.4

*Plot of mass flow rate at growth temperature as the crystal-vapour interface moves up the **calculated** temperature gradient of the growth tube, hence the smooth curve.*

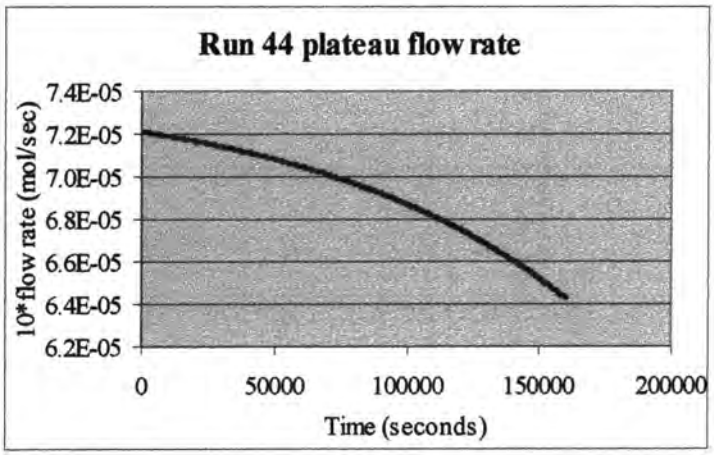

Area under plateau flow rate plot = 1.1063 moles

Fig 6.5

Mass flow rate during temperature decrease calculated from thermocouple data, again notice the exponential trend, consistent with a linear temperature decrease. The growth side temperature was calculated according to how far up the linear temperature gradient of the growth tube the crystal surface had reached.

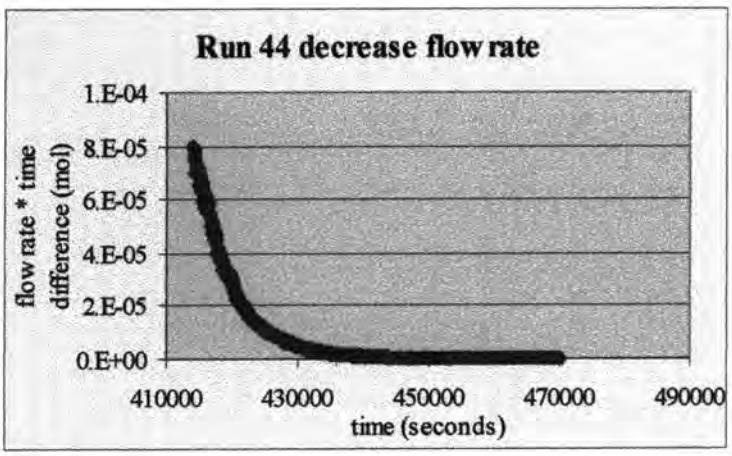

Area under decrease flow rate plot = 0.01129 moles

6.3.2 Run 41

Run 41 was conducted using the first of the growth tube designs (see sec 2.5). Due to the increased diameter of the growing surface (49mm as opposed to 29mm), and lower transport rate than run 44 or run 45, the effect of the vertical temperature gradient of the growth tube on the growth surface temperature, as the height of the boule increased was neglected. Values of P_s and P_g were calculated directly from the middle source and growth side temperatures logged during the run. As the annulus did not become blocked due to cadmium telluride condensation during the run, growth side vapour pressure conditions will be further from equilibrium than those of run 44 or run 41, making *eq 6.3* less applicable. The temperature profiles of the significant zones are shown in *fig (6.6)*.

Fig 6.6, Temperature profile of run 41 of the MTPVT system

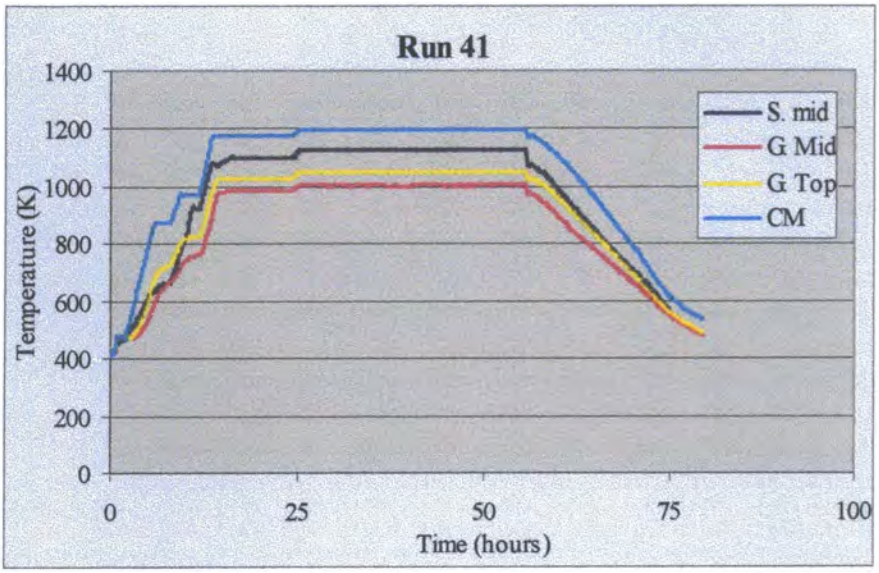

After 48 hours bakeout at 473 K, the temperature of the crossmember was ramped up in 2 stages to 900 K in order to evaporate cadmium telluride which had condensed on the crossmember at the end of the previous growth run. Again, the ramp down was staggered to prevent material re-depositing on the crossmember.

The total mass of cadmium telluride to leave the source side of the ampoule was 45.03 grams. The total mass of cadmium telluride to condense in the growth side of the ampoule was 42.69 grams. This represents a 5.2 % loss of material. This loss would be expected due to the transport of material out of the ampoule, through the annulus gap. The first growth tube design also appeared to have a sealing problem. The base pressure achieved when evacuating the ampoule prior to growth (see sec. 2.5) was somewhat higher for the first design of growth tube, due to a poorly sealing ground glass joint between the growth tube and the crossmember. There was also a large amount of material deposited on the external windows of the MTPVT system when using the first growth tube design, this problem reduced once the new growth tube, with a refitted ground glass joint, was employed.

The plot of transport rate × time interval between temperature measurements against time is shown in *fig (6.7)*.

Fig 6.7

Mass flow rate throughout run 41. The effect of the growth tube temperature gradient has been neglected due to the larger crystal diameter and lower transport rate than runs 44 and 45. The curve is not smooth due to fluctuations in temperature measurement.

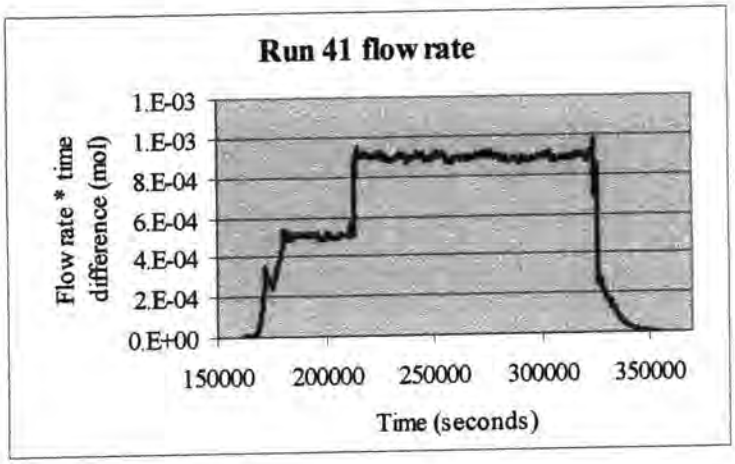

Area under run 41 flow rate plot = 0.4044 moles.

The integral of this plot is 0.40 moles. Assuming all of the cadmium telluride to leave the source side of the ampoule passed through the crossmember flow restrictor, the amount of material transported was measured as 0.19 moles. This value is 53% less than the value predicted by eq 6.2 and eq 6.3.

6.3.3 Run 45

Run 45 was conducted using the second of the growth tube arrangements. *Fig (6.8)* shows the heating profile of the run. Much higher temperatures were used during run 45. An important observation was that towards the end of growth material began to condense on the growth side ampoule viewing window. At this point, the temperature of the window (which is a cold spot due to radiative heat loss) must have been comparable to the temperature of the crystal vapour interface for CdTe to condense here rather than the growing crystal. It was assumed that at this point there would be no significant deposition on the crystal and growth was stopped.

Fig 6.8 Temperature profile of run 45 of the MTPVT system

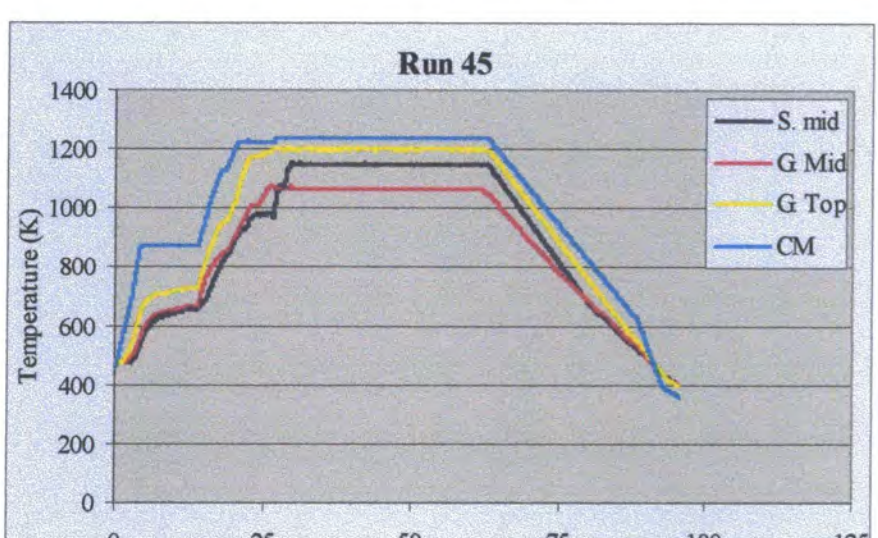

Crossmember temperature was again ramped up in stages to evaporate material from the viewing windows. The growth mid zone was ramped to temperature before the source mid zone in order to etch the surface of the crystal thermally.

The amount of material transported was calculated using the same format as *table 6.2*. Plots of flow rate × time difference between temperature measurement against time are shown for increasing temperature, the temperature plateau and decreasing temperature in *figs 6.9*, *6.10*, and *6.11* respectively.

Fig 6.9

Run 45 flow rate during temperature increase, calculated directly from thermocouple data. Notice the negative transport rate corresponding to seed temperature exceeding source temperature, this is desirable if the seed is to be thermally etched before growth.

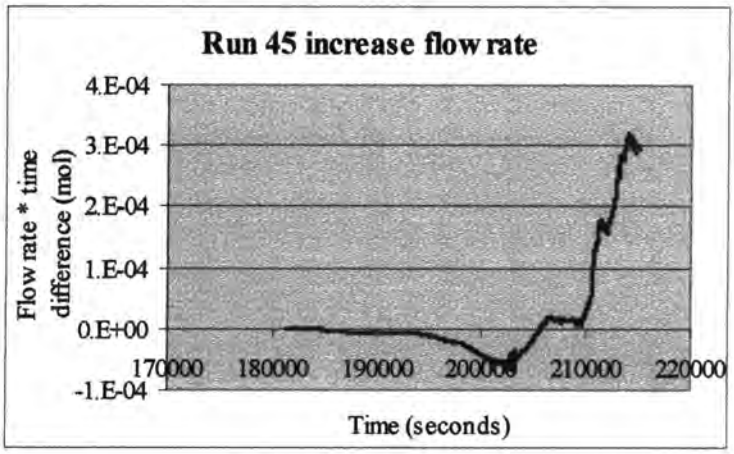

Area under increase flow rate plot = 0.01147 moles

Fig 6.10

Plot of mass flow rate at growth temperature as the crystal-vapour interface moves up the ***calculated*** *temperature gradient of the growth tube, hence the smooth curve.*

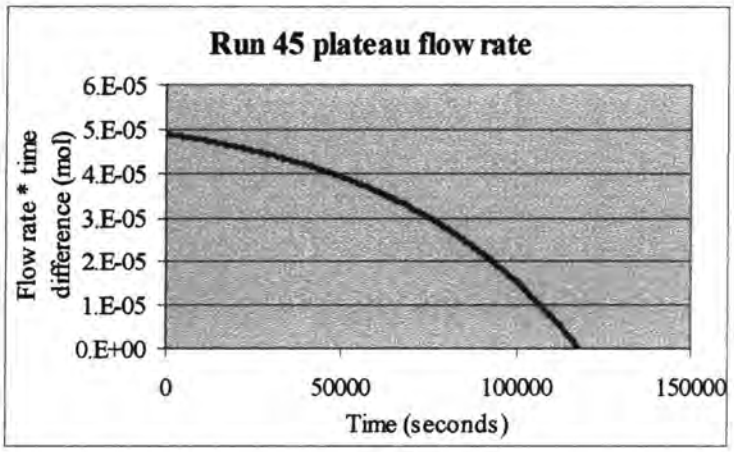

Area under plateau flow rate plot = 0.3830 moles

Fig 6.11

Plot of mass flow rate during cooldown of run 45. The plot is very noisy due to the malfunction of a source side thermocouple, which also caused a negative transport rate as the source side furnaces cooled too quickly.

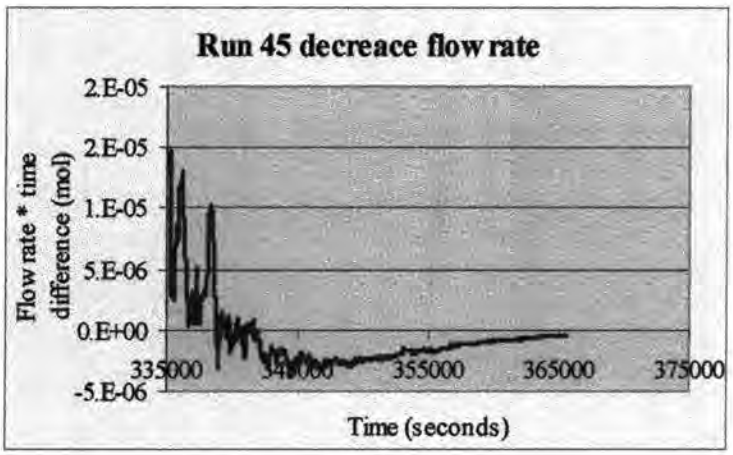

Area under decrease flow rate plot = -0.000647 moles.

Notice the negative transport during the heating up and cooling down phases. This is desirable during the heating up phase as a small amount of thermal etching before growth will help removal of any physical surface damage or any chemical layer left by the bromine methanol polishing process.

The measured mass of cadmium telluride transported was 87.01 grams, with 84.93 grams condensing in the growth side of the ampoule, this included the small amount of material which condensed on the growth side viewing window. The number of moles of cadmium telluride transported was 0.363. This compares with the predicted value of 0.394 moles, from the integration of *figs 6.9*, *6.10* and *6.11*, representing a difference of 7.9 %

6.4 Conclusion.

There is good agreement between measured transport rates and those predicted from *eq 6.2* and *6.3*, considering the approximations made, specifically concerning vapour pressure calculation and the temperature of the growing surface. This model should, in principle, allow the selection of a suitable growth rate for a given growth temperature. A fuller understanding of the relationship between vapour pressure and system temperature profile under semi-open growth conditions, using optical absorption measurements, coupled with a better control of source and growth temperatures, ideally using optical pyrometry, should allow detailed study and selection of growth conditions.

References for chapter 6

1 R. D. Present, Kinetic Theory of Gases, McGraw-Hill, New York (1958)

2 W. G. Pollard and R. D. Present, Gaseous Self Diffusion in Long Capillary Tubes, Phys. Rev., 73 (1948) 762

3 R. F. Brebrick, Partial Pressures in the Cd-Te and Zn-Te Systems, J. Electrochem. Soc.,Solid-State Sci. and Tech., 118 (1971) 2014.

Chapter 7

Conclusion and Suggestions

Chapter 7

Conclusion and Suggestions for Further Work

One of the CdTe crystals grown using the MTPVT system has been quality tested using defect revealing etching, photoluminescence measurements, and x ray diffraction analysis (*ref 1*). The results of this study were encouraging, with etch pit densities comparable with melt grown material (6×10^{-4} cm^{-2}) and relatively low strain in the crystal, as shown by x ray analysis where θ-2θ scans showed a broadening of 2 arc sec, corresponding to strains of the order 10^{-5} . Perhaps more significantly the level of strain and dislocation density reduced with growth direction, indicating and improvement in crystal quality with growth away from the cadmium zinc (4%) telluride seed where strain levels would be expected to be high due to the lattice mismatch. Photoluminescence measurements showed an acceptor bound exciton recombination peak at 1.59 eV as observed in bulk CdTe. The intensity of this peak increased with distance from the seed and the full width half maximum reduced from 4 meV at the seed to 2.1 meV at the top of the boule, again indicating an improvement in material quality with growth. Unfortunately this result has not proved easily repeatable, however this is due to technological limitations rather than the method itself. To date it has not been possible to record the vapour pressure on either side of the capillary restrictor with a high enough accuracy, due to the limitations described in chapter 3. Also, while the temperature control system provides very stable conditions during growth, heating, and cooling, the positioning of the thermocouples does not provide an accurate temperature for the crystal vapour interface or the source material, and radial temperature gradients can only be estimated from thermal

modelling of the system. Pyrometric measurement of the crystal surface (or any other method which will give the surface temperature to within 1 K and preferably allow thermal scanning of the crystal surface) is needed before the kinetics of growth can be fully investigated. Pressure difference across the capillary must also be accurately measured if transport rates are to be calculated with the required precision.

The next development stage of the MTPVT system should involve refinement of the vapour pressure monitoring system, perhaps using optic fibres to transmit light from the light source to the top of the crossmember vapour pressure monitoring windows, and likewise to transmit light from beneath the crossmember to the detectors. This would eliminate the effect of heat shield movement and CdTe deposition on the outer vapour pressure monitoring windows. The photodiode detectors should also allow different levels of pre-amplification in order to maximise the sensitivity of the lock in amplifier. Another suggestion would be the use of white light instead of cadmium light, thus avoiding having to calibrate each lamp due to the highly sensitive absorption of the 326 nm line by cadmium vapour.

The growth ampoule is transparent, allowing radiative heating and non invasive vapour pressure monitoring. This introduced complications when attempting to measure the crystal temperature pyrometrically, due to reflection from the crystal surface of radiation emitted by the optical heating elements around the crossmember. Perhaps an opaque growth tube could be used to eliminate unwanted light.

References for Chapter 7

1 N. M. Aitken, M. D. G. Potter, D. J. Buckley, J. T. Mullins, J. Carles, D. P. Halliday, K. Durose, B. K. Tanner, A. W. Brinkman, Characterisation of Cadmium Telluride Bulk Crystals Grown by a Novel "Multi Tube" Vapour Growth Technique, J. Crystal Growth, 198/199 (1999) 984

Appendix 1

Volumetric flow rate (in standard cubic centimetres per second) and the respective pressures on each side of the capillary (in mbar) for each gas tested.

Helium			Nitrogen			Argon			Sulphurhexafluride		
Rate scc/sec	A press mbar	B press mbar	Rate scc/sec	A press mbar	B press mbar	Rate scc/sec	A press mbar	B press mbar	Rate scc/sec	A press mbar	B press mbar
0.08487	0.4115	0.1029	0.09882	3.3825	1.3325	0.01605	1.3138	1.0106	0.11065	16.1241	14.4056
0.20356	2.3660	0.5144	0.28430	5.1251	1.8450	0.19565	4.2446	1.7180	0.16157	16.9329	14.6078
0.33844	3.7033	0.9258	0.47165	6.6626	2.2550	0.32015	5.4573	1.9202	0.20998	17.6405	14.6078
0.47332	4.8349	1.1316	0.65900	7.9951	2.4600	0.45525	6.5690	2.0212	0.26040	18.2471	14.6078
0.60820	5.5550	1.2344	0.84635	9.3276	2.6650	0.58240	7.4785	2.2233	0.31132	18.8536	14.7089
0.74578	6.1722	1.3373	1.03557	10.5576	3.0750	0.71750	8.5902	2.3244	0.36174	19.5613	14.8099
0.87256	7.3038	1.8517	1.22105	11.7876	3.1775	0.84995	9.4997	2.3244	0.41216	20.1678	14.9110
1.01284	8.7440	2.7775	1.40840	12.7101	3.1775	0.98240	10.4093	2.6276	0.46258	20.8755	14.9110
1.14772	9.3612	2.9832	1.59388	13.9401	3.3825	1.11485	11.4199	2.7287	0.51300	21.4820	15.1132
1.28260	10.0813	3.2918	1.78310	14.8626	3.4850	1.24995	12.4305	2.9308	0.56342	22.2907	15.1132
1.55236	12.1649	4.4330	1.97045	16.0927	3.6900	1.51750	14.3507	3.4361	0.61434	22.9984	15.3154
1.82212	13.0928	4.7423	2.15780	17.2202	3.9975	1.77975	16.1698	3.7393	0.66426	23.7060	15.4165
2.09188	14.0206	4.9485	2.34515	18.4502	4.3050	2.03935	17.7868	4.0424	0.71468	24.3126	15.5176
2.35894	14.9485	5.1546	2.53250	19.5777	4.5100	2.30690	19.6059	4.3456	0.76560	24.9191	15.5176
2.63140	15.7732	5.3608	2.71985	20.6027	4.7150	2.56915	21.3239	4.5478	0.81552	25.5257	15.6187
2.90116	16.7010	5.6701	2.90907	21.7302	4.9200	2.83935	23.0419	4.9520	0.86594	26.1322	15.6187
3.17092	17.6289	5.9794	3.09642	22.8577	5.1251	3.12544	24.9621	5.2552	0.91686	26.8399	15.7198
3.44068	18.6598	6.3918	3.28190	23.8827	5.3301	3.36120	26.3770	5.5584	0.96678	27.5475	15.9220
3.71044	19.4845	6.7010	3.46738	25.0103	5.6376	3.62875	28.0950	5.8615	1.01720	28.1541	16.0230
3.97750	20.4124	7.0103	3.65847	26.0353	5.8426	3.89895	29.8130	6.1647	1.06712	28.6595	16.0230
4.25266	21.2371	7.2165	3.84582	27.1628	6.1501	4.16120	34.2945	8.9598	1.11804	29.2661	16.1241
4.51972	22.2680	7.7320	4.03317	28.1878	6.3551	4.42875	35.8393	9.5778	1.16846	29.9737	16.1241
4.78948	23.1959	8.1443	4.21865	29.3153	6.5601	4.70160	38.1050	10.1957	1.21888	30.6814	16.2252
5.05924	23.9175	8.2474	4.40413	30.3403	6.6626	4.96120	39.9588	10.4016	1.26930	31.2879	16.3263
5.32900	24.6392	8.6598	4.59522	31.3653	6.8676	5.22080	41.6066	10.7106	1.31972	31.9956	16.5285
5.59876	25.4639	8.7629	5.53010	36.6954	8.0976	5.48570	43.2544	11.1226	1.37014	32.6021	16.5285
5.87122	25.6701	8.3505				5.75325	44.5045	10.1903	1.42056	33.1076	16.7307
6.13828	26.5979	8.8660				6.01550	45.7523	10.1903	1.47098	33.8152	16.6296
6.40804	27.2165	9.1753				6.28305	47.3121	10.2943	1.52140	34.5228	16.7307
									1.77350	37.8589	17.3372
									2.02560	41.0938	18.0449

Appendix 2

Spreadsheet formulae used to calculate mass transport from ch 6

A	B		C
1	Notes:-P(t_start(K)) = growth temp		
2	growth temp = p(t_start(K))+qt (where t=1~t_{max})		
3	K_v, K_m = viscous+molecular constants		
4	l_s =a-bp		
5	m_s = bq		
6	n_s = cp		
7	r= cq		
8	q=delta T/t_{max}		
9	P_g=A(exp-((a-bt)/ct))^2/3		
10	rate = K_vP_s^2/(T_c)+ K_mP_s/sqrt (T_c) - K_vP_g^2/(T_c)- K_mP_g/sqrt (T_c)		
11	K_o = P_s components of rate equation.		
12	K_v	0.04723176716*((C17^4)/(C18*C13))	A=1.26
13	K_m	((0.06439683103*(C17^3))/C18)*169.043	P(t_start(K))=1003
14	q	(C19-C13)/C23	P_s(Pa)=670
15	l_s	C20-(C21*C13)	Visc (Pa.S)=9.00E-5
16	m_s	C21*B14	T_c (K)=1198 crossmember temp.
17	n_s	C22*C13	r(m)5.20E-4
18	r_s	C22*B14	L(m)=1.17E-2
19	K_o	((B12*C14^2)/C16)+((B13*C14)/(SQRT(C16)))	T_{gmax}(K)=1073
20			a=6.9446E+4
21			b=45.82
22			c=1.9872
23			T_{max} (s)= 160000
24	No mol=	SUM($C28:$C16028)	
25			
26	Time (s)	Growth Press (Pa)	10*flow rate
27			
28	1	100000*($C$12*((EXP(-($B$15-($B$16*A28))/($B$17+($B$18*A28))))^(2/3)))	10*(($B$19)-(($B$12*B28^2)/$C$16)-(($B$13*B28)/SQRT($C$16)))
29	11	100000*($C$12*((EXP(-($B$15-($B$16*A29))/($B$17+($B$18*A29))))^(2/3)))	10*(($B$19)-(($B$12*B29^2)/$C$16)-(($B$13*B29)/SQRT($C$16)))
30	21	100000*($C$12*((EXP(-($B$15-($B$16*A30))/($B$17+($B$18*A30))))^(2/3)))	10*(($B$19)-(($B$12*B30^2)/$C$16)-(($B$13*B30)/SQRT($C$16)))
31	31	100000*($C$12*((EXP(-($B$15-($B$16*A31))/($B$17+($B$18*A31))))^(2/3)))	10*(($B$19)-(($B$12*B31^2)/$C$16)-(($B$13*B31)/SQRT($C$16)))

Up to 160000 seconds

Sample data evaluated using the above spreadsheet.

Run 44.							
Plateau Integra	1.10634						
Increase Integr	0.03125						
Decrease Integ	0.01129						
Total	1.14889						
	Plateau						
Time(s)	Pg(pa)	10*flow rate(mol)					
1	48.7971	7.2E-05					
11	48.8021	7.2E-05					
21	48.807	7.2E-05					
31	48.812	7.2E-05					
41	48.8169	7.2E-05					
51	48.8219	7.2E-05					
61	48.8268	7.2E-05					
159951	221.977	6.4E-05					
159961	221.997	6.4E-05					
159971	222.016	6.4E-05					
159981	222.036	6.4E-05					
159991	222.056	6.4E-05					
160001	222.075	6.4E-05					
	Increase						
Time(s)	S. Mid(C	G. Mid(C	CM(C)	S press(Pa	G Press(Pa)	Rate*time period(mol)	
200001.02	634.77	553.16	683.18	4.266991	0.3381304		
200061.77	634.42	553.36	683.42	4.224959	0.3404461	1.002E-06	
200117.85	635.87	553.58	683.67	4.401612	0.3430103	9.664E-07	
200178.65	635.14	553.73	683.95	4.311843	0.344769	1.024E-06	
253701.68	847.46	729.07	923.28	557.0789	47.755958	0.0001688	
253757.87	852.71	729.52	923.64	613.8066	48.256951	0.0001778	
253818.56	836.05	729.67	923.7	449.7925	48.425013	0.0001254	
253879.36	836.51	729.97	924.11	453.7271	48.762743	0.000127	
	Decrease						Rate*time
Time(s)	S. Mid(C	G. Mid(C	G top(C	CM(C)	S press(Pa)	G Press(Pa)	period(mol)
414018.32	843.14	725.59	793.32	920.38	514.00237	193.83107	
414079.12	842.74	725.37	792.95	920.06	510.17029	192.36664	0.0001105
414139.87	842.37	724.97	792.5	919.73	506.64864	190.59912	0.0001095
414200.51	841.69	724.53	792.09	919.43	500.2337	189.00157	0.0001073
469821.85	452.79	389.54	449.26	561.45	0.0068457	0.0058517	2.754E-10
469878.15	452.26	389.27	448.86	561	0.006687	0.0057481	2.395E-10
469939.29	451.77	388.97	448.43	560.62	0.0065433	0.0056385	2.507E-10
470000.03	451.41	388.69	448.02	560.08	0.0064396	0.005536	2.488E-10